2019-01-01

Tailoring Physical Properties Of Shape Memory Polymers For FDM-Type Additive Manufacturing

Paulina Aileen Quinonez
University of Texas at El Paso

TAILORING PHYSICAL PROPERTIES OF SHAPE MEMORY POLYMERS FOR FDM-TYPE ADDITIVE MANUFACTURING

PAULINA AILEEN QUIÑONEZ

Master's Program in Metallurgical and Materials Engineering

APPROVED:

David A. Roberson, Ph.D., Chair

Binata Joddar, Ph.D.

Reza Ashtiani, Ph.D.

Stephen L. Crites, Jr. , Ph.D.
Dean of the Graduate School

For my family & friends who supported and encouraged me through this journey…

TAILORING PHYSICAL PROPERTIES OF SHAPE MEMORY POLYMERS FOR FDM-TYPE ADDITIVE MANUFACTURING

by

PAULINA AILEEN QUIÑONEZ, B.S.

THESIS

Presented to the Faculty of the Graduate School of

The University of Texas at El Paso

in Partial Fulfillment

of the Requirements

for the Degree of

MASTER OF SCIENCE

Department of Metallurgical, Materials and Biomedical Engineering

THE UNIVERSITY OF TEXAS AT EL PASO

December 2019

Acknowledgements

I would like to give thanks to Dr. David A. Roberson for allowing me to be a part of his lab, it meant so much to me to have a helping hand that was willing to go above and beyond for his students. Not only did I gain a mentor and an advisor but throughout this whole journey I ended up gaining a friend, I am truly grateful for this opportunity and the wonderful moments I got to spend in the lab.

I want to thank my parents for being great role models and supporting me in my career. I have learned so much from you and I am proud to call them my parents, I hope that I've made you proud and this victory is as much yours as it mine. To my mother who is my hero, who has shown me to be strong and be persistent in reaching my goals and never giving up. She is the reason for the person I am today and I am greatly thankful that she has always stood my by side and guided me, even when I though I didn't need it. She is my inspiration in life and I wish there was a way to thank her for all she has done for me because she has given my brothers and I the best life.

I want to acknowledge my brothers, Alan and Ivan Quinonez, because I truly got lucky with these incredible men as my brothers. I hope that I've made you proud to have me as a sister and this accomplishment is one we share because it's because of you guys that I am able to follow my dreams. Your encouragement and love have really helped me in this whole process and you guys more than anybody have put up with me and have never let me down. I am incredibly proud to have you as my brothers because as you've come to grow, you have become exceptional people who I am so proud of and I know that no matter what happens in this world, we will always have each other's back.

Paulina & Leticia, I really could not have done this without you girls and I am truly grateful for all the support and encouragement you girls provided. I really did get lucky by having you two as my mentees and I wouldn't have picked any other people from the department or the school for that matter, to experience this journey with. I want to thank you from the bottom of my heart for your efforts and for keeping the lab laughing throughout the whole year. Not only did I get the

chance to be a mentor to both of you, but after this journey I can honestly say that I gained two new incredible best friends. I wish you the best in your future endeavors and I know that whatever you set your minds to, you girls will accomplish because I've gotten to know two brilliant, intelligent, brave, and funny girls, whom I wish the best of this world to.

I was to thank Diego Bermudez for being an incredible friend and lab mate, I could not have finished this thesis is if wasn't for your help and encouragement. I am truly grateful for having such a wonderful person in my life as you and I know that no matter what you decide to do in life you will be successful because you are a great role model for others. Danisha Rivera, I want to thank you for all you have done for me, it is because of you that I decided to embark on the journey of doing my master's. You were an incredible mentor and I learned so much from you that you encourage me to be the best I can and to never give up on anything I really want. I am so happy to call you my friend and thank you for guiding me throughout all these years. Mauro Ruiz, Anahy Martinez and Cristina Azcarate, thank you for listening to me when I needed to blow off steam, I really couldn't have done it without my best friends. I am truly grateful for you all, for standing with me when I needed you most. I know that I have not only found incredible friends, but a second family. Thank you for your support and encouragement through this process and for always listening.

Elsy, Karla, Alejandra and Paulina, thank you girls for being a huge part of my life. I want to thank you for listening and always being there for me when I needed it the most. I hope that I have made you proud and that our friendship will continue to flourish through the years. I have been lucky to have you girls as my best friends for about 15 years and counting.

I would like to thank my aunts for being the best role models in my life and for being like mothers to me. This is for all of you, I hope that I've made you proud and thank you for your encouragement and love. I got lucky to have such incredible women in my life whom I look up to. I also want to thank my grandma Maria de los Angeles Castaneda, she is the reason why I decided

to follow my dreams and continue my education. She encouraged me to be the best person I can be and to never give up, to be brave and stand up for myself when I needed it. Her life stories taught me that no matter what happens in life, as long as were willing to stand up and continue, there is always a better tomorrow.

I would also like to thank my fellow lab mates, who made a great working environment in the lab and whom not only I got the pleasure to work with but I became friends with. Thank you the encouragement, laughs and the fun times. Thank you to Estebanne, Truman, Rhyan, Gwon, Ariana and Arlene, you were the best people to work with.

Abstract

Shape memory polymers (SMPs) have found applicability in biomedical settings as well as other uses that can take advantage of objects that can change shape upon exposure to stimulus. Integrating polymers with shape memory characteristics into additive manufacturing technologies such as fused deposition modeling (FDM™) can increase the number of applications this manufacturing platform can be utilized. Currently, polyurethane and polylactic acid (PLA) are two FDM™-compatible materials that possess shape memory properties. On their own these materials do not have tunable shape memory properties, namely shape recovery and shape fixation. The work presented here entails the development and characterization of two shape memory polymer material systems intended for FDM™-type additive manufacturing platforms. Here, two polymers with differing shape memory mechanisms (dual component and dual state) were combined in iterative ratios leading to material systems with tunable physical properties. Specimens fabricated via fused filament fabrication (FFF) were compared to those fabricated via injection molding. Dynamic mechanical analysis (DMA) was used to determine the critical thermal and rheological parameters as well as determine shape recovery temperature. Characterization of polymer crystallinity was determined via X-Ray diffraction (XRD) while scanning electron microscopy (SEM) was used to characterize the fracture morphology of impact test specimens. The shape memory properties were determined by deforming the specimens at room temperature and then recovering in an oven at a temperature corresponding with the maximum tan δ temperature. Of the material systems that could be evaluated by room temperature deformation, nearly 100% shape fixation and shape recovery was observed.

Table of Contents

List of Tables

List of Figures

Chapter 1

Background

Additive manufacturing (AM) has generated a great amount of interest over the past two decades due to the ability to shorten the design to product cycle time, ability to fabricate complex geometries that could not otherwise be realized, and the capability to provide on demand manufacturing. As interest in AM has grown, so too has the advancement of technologies based on this manufacturing technique where the feedstock is metals, polymers or ceramics. The advancements of these technologies depend significantly on the availability of materials that possess a wide range of physical properties compatible with a given AM technology. An interest in fused deposition molding (FDM™) technology has increased due to its ease of use, its low cost, and the readily material available for 3D printing objects, which in this case, is in the form of a thermoplastic filament. Additive manufacturing systems based on FDM™ technologies; also known as fused filament fabrication (FFF) and material extrusion additive manufacturing (MEAM), can now be found in academic, industrial as well as home-user settings (Berman, 2012; Chulilla Cano, 2011; Perez et al., 2014) A need for the development of new materials that possess specific desired properties is required due to the common use of this technology in today's society. The development of new materials greatly benefits FDM™-type AM because it allows for high scalability of 3D printed objects that could be implemented into applications such as electronics and biomaterials (Buyuksungur et al., 2017; Esposito Corcione et al., 2017; Shemelya et al., 2017). FDM™-type AM technologies are composed of two strategies that are generally employed: 1) the creation of new polymer blends; and 2) the creation of new polymer matrix composites (Roberson, Shemelya, et al., 2015). Taking this into consideration, a third strategy would be to understand and

study these polymers to find if they can be utilized in different process manufacturing methods, such as their applicability to FDM™-type manufacturing—as was the case with NinjaFlex®, a thermoplastic urethane (TPU) that was originally developed by Fenner Drives, Inc. to serve as belts in automated teller machines (ATM)s. The premise of developing new materials for FDM™-type AM platforms becomes more profound if a system with tunable properties is developed. An example of a thermoplastic composite system with tunable X-ray shielding capability was demonstrated by Shemelya et al. (Shemelya et al., 2015) where the shield capability of polycarbonate was manipulated by varying the content of tungsten within the composite. Here, the material system was compatible with desktop-grade FFF 3D printers and the intended application was to protect electronic systems in CubeSat satellite systems. An example of a FFF-compatible polymer blend system was made by Siqueiros et al. (Siqueiros et al., 2016) who demonstrated the development and characterization of rubberized acrylonitrile butadiene styrene (ABS) blends. Multiple grades of ABS were combined with the thermoplastic rubber (TPR) styrene ethylene butylene styrene (SEBS) in different weight ratios in the creation of a material system with tunable rigidity. Ternary blends composed of ABS, SEBS and ultra-high molecular weight polyethylene (UHMWPE) were demonstrated by Rocha et al. (Rocha et al., 2014) .

A shape memory alloy is characterized as a smart material that has a shape memory effect (SME) due to their ability to deform by heating at different temperatures and regain their shape by cooling. Further development of this technology has generated interest in shape memory polymers (SMP) because it allows control of obtaining specific properties that would enhance the materials use in different applications. Development of shape memory polymers (SMP) has gained attention due to its innovative uses for development in different areas that could replace materials that are

more expensive and more difficult to obtain. SMPs are known as self-repairing smart materials due to their ability to nearly regain their original shape after deformation. Lendlein A. et al. (Lendlein et al., 2005) explained that SMPs could be an excellent alternative to replace shape-memory alloys due to their low cost and easy accessibility of material. Here, a new type of technology, such as the SMP, is presented to showcase the development of new materials. These materials show to have enhanced properties and use in many fields such as biomedical, environmental and electronics. The SMP technologies have gotten interest due to the material's ability to deform at different temperatures, having specific desired properties, low weight and low density. Luo et al. (Luo and Mather, 2013)indicated that although SMPs are an advancing technology and have matured in a short time, there is still a need for further development. There is still a need for new materials with specific requirements that are needed to help develop new medical devices. Figure 1.1 shows a picture demonstration of the shape memory effect of a material. The material is heated to its deformation temperature for a permanent shape, then its heated again to its recovery temperature and it regains its original shape.

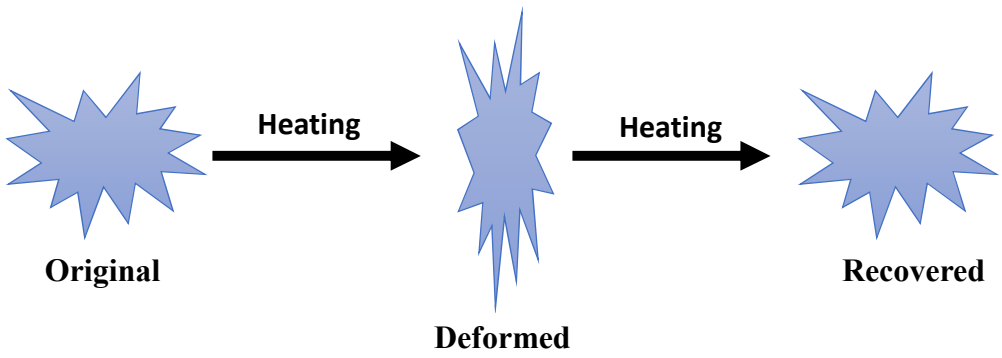

Figure 1.1 Depiction of the shape memory effect in a material.

Materials that have been studied for this type of SMP technology have not been manufactured or studied for AM technologies. The work presented here will showcase the ability of SMP material blends to be used for FDM-type AM. The materials that were chosen are known to possess great shape memory properties although they differ in the mechanism that drives their shape memory effect and makes them shape memory polymers. Here, two types of materials were combined, one which is a dual state mechanism polymer and another two which are dual component mechanism polymers.

Polylactic acid (PLA) has been of great interest due to its accessibility, biocompatibility, non-toxicity and the fact that it is biodegradable. This material possesses biomedical and environmental applications and if combined with other materials. It could be implemented into electronics as is the hope for further development of this material. While PLA has promising properties, it should be noted that it cannot be stretched at room temperature and therefore, requires a material that can help enhance its properties. Thermoplastic urethane (TPU) and styrene ethylene butylene styrene (SEBS) are rubber-like materials with elastic properties that also demonstrate shape memory properties caused by their ability to regain the shape of their original material. The issue with these materials is that, because of their "rubbery" nature, they cannot withstand to hold a deformation because they automatically return to their given shape. Figure 1.2 illustrates the three (3) different polymers that will be used to create two blends, which will be characterized to understand their properties, as well as study their manufacturing process and how they affect the SMP technologies. To develop a material that has good shape memory properties, it should be noted that a material must have a high recovery strain and recovery ratio, these are special characteristics of SMP's.

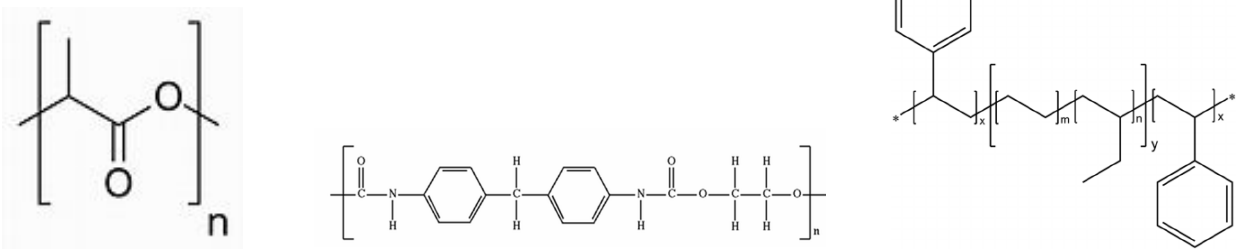

Polylactic Acid (PLA) | Thermoplastic Urethane (TPU) | Styrene Ethylene Butylene Styrene(SEBS)

Figure 1.2 The chemical composition of the three polymers that will be used in this study.

The shape memory properties of variants of the ABS-SEBS blends first developed and presented in Siqueiros et al. (Siqueiros et al., 2016) were explored by Chávez et al. (Chávez et al., 2018) where it was found that shape memory values, namely shape fixation ratio (R_f) and shape recovery ratio (R_r) varied with the composition of SEBS content. Additionally, it was reported that these shape memory properties differed depending on the print raster pattern. In this prior work and additional studies pertaining to shape memory polymers performed by others (Alan Schoener et al., 2010; Lai and Lan, 2013a; Memarian et al., 2018), R_f and R_r are calculated as follows:

$$R_f(\%) = \frac{\varepsilon_u}{\varepsilon_m} \times 100\% \qquad (1)$$

$$R_f(\%) = \frac{\varepsilon_m - \varepsilon_p}{\varepsilon_m} \times 100\% \qquad (2)$$

where deformation is performed in a tensile testing machine and ε_u is the elongation of the specimen after the load is removed, ε_m is the maximum strain the specimen is subjected to (usually

100% elongation) and ε_p is the elongation of the specimen after recovery. In most cases involving thermoplastic shape memory polymers, recovery is achieved by heating the specimens. Overall, shape memory effect can be assessed by the shape memory index (SMI), which is a combination of the two parameters calculated above and attained by the following equation (Chávez et al., 2018; Lai and Lan, 2013b):

$$SMI(\%) = (R_r \times R_f) \times 100 \qquad (3)$$

Chavez et al. performed a study that characterized the shape memory chacteristics of the ABS:SEBS material system mentioned above. While originally developed for AM processing, the blend was not necessarily designed with intentions of using it as a shape memory material. Although intentions were not related to SMP applications, it was demonstrated that two iterations of the ABS:SEBS blend (50:50 and 25:75 by weight ratio ABS:SEBS) possessed shape memory characteristics meaning that a shape memory polymer that was compatible with FDM™-type AM platforms had been sucessfully developed. Key aspects of this previous work include: 1) finding that the polymer phases aligned due to the printing process; 2) the shape memory characteristics were dependent on raster pattern; and 3) that dependence of either R_f and R_r on raster pattern changed depending on deformation temperature

The shape memory effects of polymeric materials are classified by three of mechanisms as described by Yang et al. (Yang et al., 2014). The first mechanism, the dual state mechanism, is where the shape memory effect is driven by strong crosslinks (covalent bonds) that holding on the the permentant shapeand weak crosslinks (chain entanglement, for example)) that hold the tempoary shape. The second mechanism, dual component, is one where the shape memory effect

is driven by hard and soft components. The hard components that can be either on the molecular or micro scale. Finally, the third mechanism is the partial transition, where a mixture of two materials – one of which changes phases – controls the shape memory effect where the example given by Yang et al. was a compressable sponge infultrated by parafin wax.

Of the three mechanisms governing shape memory polymers, the study presented in this thesis will focus on two of the mechanims due to the nature of the materials that were chosen – one that has dual state and two materials that have dual component mechanisms. The dual state mechanism is seen in PLA, where there is a temporary shape maintained by the weak cross-links present within the polymer. These cross-links act as an element able to store elastic energy,which is the driving for later recovery within the material, as mentioned in Yang et al. (Yang et al., 2016) This property accounts for the "remembered" shape by the strong cross-links (due to covalent bonding). The dual component mechanism is seen in SEBS and TPU. This materials mechanism comes from hard and soft components, and the "remembered" shape is governed by the hard components, while the soft components determine the temporary shape of the material. The hard component of this material is the elastic part that works with different temperature ranges, and the soft component becomes soft when the material is heated,thefore allowing the deformation to take place. The SEBS and TPU component maily deforms at high temperatures. This will help determine which mechanism is better for shape memory demonstrations. Figure 1.3 illustrates an image indicating the difference between the two mechanisms.

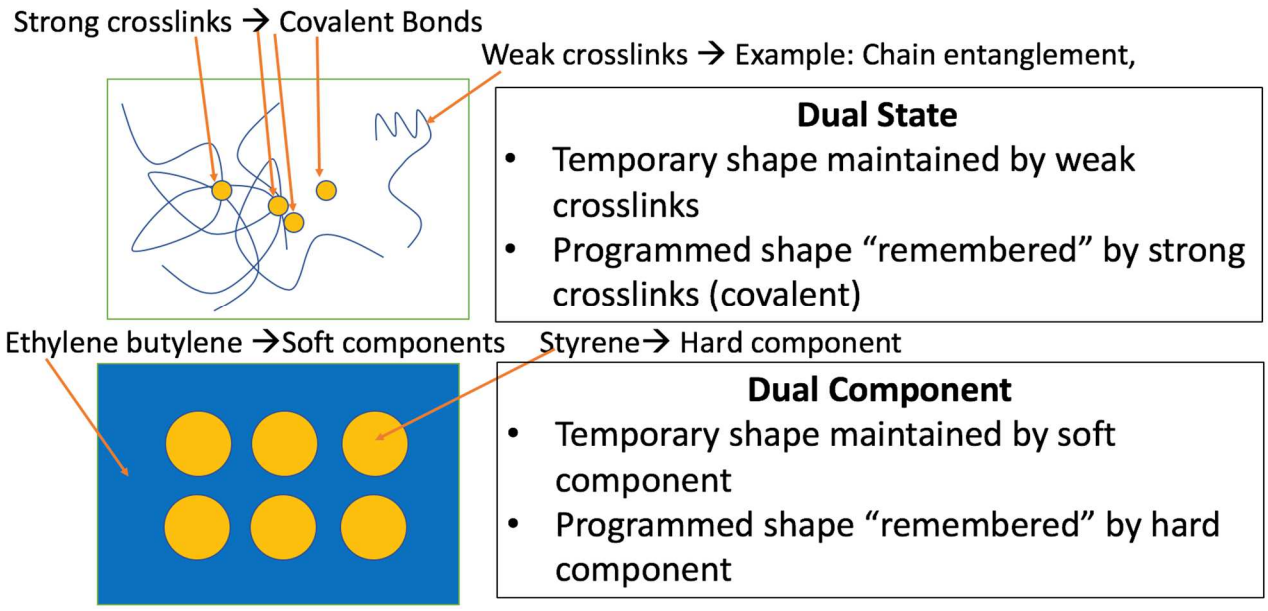

Figure 1.3 Depection of difference between dual state and dual component mechanisms.

The analysis presented in this study will illustrate the characterization of two material blends – PLA combined with SEBS and PLA combined with TPU at different weight ratios. Characterization of these two new material blends helped study their behavior and determining the properties that enhance shape memory in the polymer. These materials will be characterized by dynamic mechanical analysis (DMA), X-Ray diffraction (XRD), impact testing, scanning electron microscopy (SEM) to analyze the fracture surface, and tensile testing which will determine which blends can withstand shape memory deformation at room temperature. S.-M. Lai and Y.-C. Lan (Lai and Lan, 2013a) mentioned that the early development of shape memory polymers (SMP) exhibited a block copolymer that had a hard domain which was representative of the revisable phase and a soft block that was representative of the switch phase for the effect of shape memory polymers. This gives indications of a material having the ability to deform at a given temperature and, by switching the temperature, the material will regain its original shape. There are two components that are required to show that a material has good shape memory effect which are a

good shape fixing ratio and a good shape recovery ratio. These two will demonstrate that a material has the ability to be considered for future development in use of shape memory technologies.

In this work, the materials chosen with different shape memory mechanisms in order to ascertain which type would contribute more to the overall shape mempry effect of resultant polymer blend. Polylactic acid (PLA) posesses shape memory characteristics driven by the dual state shape memory effect, while SEBS and TPU have a shape memory effect driven by the dual component mechanism. Considering these materials demonstrate different mechanisms that drive their shape memory effect, PLA:SEBS blends and a PLA:TPU blends with different weight ratios were made. The overall scope of this project entails the use of two elastomeric materials. These two different elastomeric materials were chosen because a need to explore what their effects of miscbility are on the overall shape memory effect. Solubility parameters for these types of materials will help understand how well both materials will mix with PLA. PLA and TPU would be expected to blend well together due to demonstration that their solubility parameters (δ) are similar with values of roughly 20 to 20.5 $MPa^{1/2}$ (Siemann, 1992; Wang et al., 2018). In contrast, polystyrenes and SEBS have solubility parameters of roughly18.3 and 17 $MPa^{1/2}$ (Peng Wu et al., 2011) , repectively, so it was expected that the result of combining SEBS with PLA would result in an imiscible blend. Pantoja M. et al. (Pantoja et al., 2019) mentions that thermoplastic elastomers are known to microphase separatly which results in immiscibility. This is mainly due to their polystyrene (PS) and midblocks, which are creating lamellar domains that are functions of the PS content. Additionally, the previous work presented in Chávez et al. revealed the ABS-SEBS blend to be an immiscible blend by way of scanning transmission electron microscopy (STEM), which also indicated that the varouis phases aligned with the print direction. The imiscibility was

predictable as ABS has a solubility parameter ranging from 20 to 23 $MPa^{1/2}$ (Peng et al., 2010) and it was hypothesized that the alignment of the imiscible phases had an effect on the shape memory parameters and their dependence on raster pattern. In the work presented here, it was thought that, by creating miscible and immiscible blends, the effect of phase alignment on the shape memory process could be deconvoluted from the well-known effect of print raster on mechanical properties, which has been documented heavily in literature (Es-Said et al., 2000; Perez et al., 2014; Torrado et al., 2015; Torrado and Roberson, 2016; Vega et al., 2011). The work presented here is the characterization of novel shape memory materials intended for use in FDM-Type additive manufacturing platforms. Here, we present the characterization of different material blends developed with the intent of creating shape memory polymeric systems that are compatible with FFF printers.

Other investigators have worked with similar material systems. The shape memory effect of adding a polyimide elastomer (PAE) was documented by Zhang et al. (Zhang et al., 2009) Key findings in this work were that the PAE was exhibited some level of miscibility with PLA and that the addition of PAE to PLA enhanced the inherent shape memory properties of PLA due to overcoming the native brittleness of PLA. The work involving PAE is relevant to this study because PAE is similar to TPU. Blending of SEBS with PLA has been carried out by other researchers as well where SEBS demonstrated an ability to toughen PLA through a rubber toughening mechanism, and also enhanced PLA's resistance to heat (Hashima et al., 2010; Jiang et al., 2013). The work presented in this work differs from prior work on the same systems in that AM was not a component of these prior works. Additionally, we have found no work that has explored the shape memory properties of PLA:SEBS.

In this study, we present the shape memory effect of the two different blends, PLA:SEBS and PLA:TPU in comparison to different raster patterns and injection molding. This demonstration will showcase how certain blends will be able to recover nearly to their original shape by pulling tensile specimens at room temperature. The intent of this analysis is to make a comparison of mechanisms to elucidate whether dual-state or dual-component is the more dominant mechanism that drives for a better shape memory effect.

Chapter 2

Experimental Methods

PLA grade 4043D was combined with four weight percentages (5%, 10%, 25%, 50%) of styrene ethylene butadiene styrene with a maleic anhydride graft (SEBS-g-MA grade FG1901-GT, Kraton, Houston, TX, USA). Extrusion of a filament with a diameter of 2.85 +/- 0.05 mm was obtained using Collin twin screw extruder/compounder Model ZK 25T (Collin Lab and Pilot Solutions, Norcross, GA, USA). Later, filaments were dried using VWR Forced air oven 3.65 (VWR International, PA, USA) at 80°C for 4 hours.

Tensile test specimens were 3D Printed using a Lulzbot TAZ 5 outfitted with an SE Aerostruder with a 0.5mm nozzle (Aelph Objects Inc., Loveland, CO, USA) following the ASTM Standard D638 in accordance with the Type V specimen geometry. The tensile test specimens were printed in a 45° and longitudinal raster patterns with the print raster perpendicular and parallel, respectively, to the direction of applied stress. The samples were printed with an infill of 100%. The impact specimens were also printed on Lulzbot systems, however a crosshatched raster pattern (alternating 45° layers in the XYZ direction) was used. The printing temperature of the blends increased as the weight percentage increased, therefore to improve bed adhesion Elmer's Glue Stick was used. Impact specimens were obtained using Lulzbot Taz 5 FlexyDually (Aelph Objects, Inc., Loveland, CO, USA) following ASTM Standard D256-10 in the XYZ direction with a 45° raster pattern and printed stress concentrator. The build orientation was chosen because it was demonstrated by Roberson et al. (Roberson, Torrado Perez, et al., 2015) that this orientation has the greatest resistance to impact. Printing parameters for the materials are listed in Table 2.1. Tensile and impact specimens for each blend were also prepared by injection molding by using an

LNS Technologies manual injection molder (Model 150A, LNS Technologies, Scotts Valley, CA, USA)where the processing temperatures are listed in Table 2.2. A portion of the extruded filament was pelletized with a Strand Pelletizer (Collin Lab and Pilot Solutions, Norcross, GA, USA) and dried a Gravity Convection Oven (Model??? VWR®) to be used for the injection molding of both tensile and impact test specimens. The material was heated to its corresponding temperature, in which we converted °C to °F using their printing temperatures for accuracy and once the pellets were heated, we injection molded the material unto a molding for each given specimen. A total of 6 specimens was created for each material type for tensile testing, impact testing and shape memory property characterization.

Table 2.1 Printing parameters for 3D printed specimens of PLA/TPU and PLA/SEBS.

	PLA:TPU				**PLA:SEBS**			
Ratio	5:95	10:90	25:75	50:50	5:95	10:90	25:75	50:50
Printing Temp.	205°C	212°C	225°C	250°C	205°C	210°C	225°C	260°C
Bed Temp.	60°C	60°C	60°C	60°C	60°C	60°C	60°C	60°C
Nozzle Diameter	0.6 mm	0.6 mm	0.6 mm	0.6 mm	0.6 mm	0.6 mm	0.6 mm	0.6 mm
Fill Percentage	100%	100%	100%	100%	100%	100%	100%	100%
Primary Layer Height	0.2 mm	0.2 mm	0.2 mm	0.2 mm	0.2 mm	0.2 mm	0.2 mm	0.2 mm
Printing Speed	30 mm/s	30 mm/s	30 mm/s	30 mm/s	30 mm/s	30 mm/s	30 mm/s	30 mm/s
Filament Diameter	2.85 mm	2.85 mm	2.85 mm	2.85 mm	2.85 mm	2.85 mm	2.85 mm	2.85 mm

Table 2.2 Printing parameters for injection molding specimens of PLA/TPU and PLA/SEBS.

	PLA:TPU				PLA:SEBS			
Ratio	5:95	10:90	25:75	50:50	5:95	10:90	25:75	50:50
Printing Temp.	375°F	375°F	390°F	390°F	375°F	375°F	390°F	390°F

Mechanical properties of the compounded material systems were obtained through a variety of testing methods. Dynamic mechanical analysis (DMA) was performed using a PerkinElmer Model DMA 8000 (PerkinElmer, Waltham, MA, USA). The average dimensions of the specimens were the following, length of 40 mm, width of 8 mm and thickness of 2 mm. Dual cantilever mode was used for testing of the specimens. The temperature scan ranged from -40°C to 110°C at a rate of 5°C/min. X-Ray diffraction was carried out through the use of a Bruker D8 Discover X-Ray Diffractometer (Bruker Scientific LLC, Billerica, MA, USA). Izod impact testing was performed using Tinus Olsen Model IT 504 (Tinus Olsen, Horsham, PA, USA). The impact testing was carried out with a nominal weight of 1553.5 +/- 7.6 grams and latched pendulum potential energy of 7.44 Joules. Horizon software was used to determine the impact resistance, impact strength, and specimen break type.

Fracture surface analysis of spent impact test specimens was performed with a Hitachi SU-3500 (Hitachi America, Ltd, New York USA) scanning electron microscope. To reduce the effect of charging, the SEM was operated in variable pressure mode operating at 90 Pa and images were acquired through the use of a backscatter electron (BSE) detector or an ultra-variable detector (UVD). Tensile testing of the printed specimens was performed using MTS Criterion C-44 (MTS

Systems Corporation, Eden Prairie, MN, USA) and carried out at a constant strain rate of 10mm/min. Properties such as ultimate tensile strength (UTS) were obtained.

Table 2.3 Specimen number for each characterization technique used in this study.

BLENDS	3D Printed PLA/SEBS				3D Printed PLA/TPU				Injecting Molding SEBS-TPU			
%	5 %	10 %	25 %	50 %	5 %	10 %	25 %	50 %	5 %	10 %	25 %	50 %
DMA	1	1	1	1	1	1	1	1	-	-	-	-
Impact	2	2	3	3	3	3	3	3	3	3	3	3
XRD	2	2	2	2	2	2	2	2	-	-	-	-
SEM (Fracture surfaces)	4	4	4	4	4	4	4	4	4	4	4	4
Tensile	3 45° 90°	3 45 90°	3 45° 90°	3 45° 90°	3 45° 90°	3 45° 90°	3 45° 90°	3 45° 90°	3-3	3-3	3-2	3-2

Tensile testing was used as a stopgap to determine which blend compositions were suitable for shape memory characterization. The selection criteria was simple: If the sample pool of tensile test specimens could sustain greater than 100% elongation, then that particular composition would be subjected to shape memory property characterization. While deformation at an elevated temperature near the glass transition temperature (T_g) is the norm, the means to deform the specimen at an elevated temperature were not available so deformation was carried out at room temperature. It is noted here that the 45° raster pattern was not found suitable for shape memory characterization at any temperature as delamination occurred as seen in Figure 2.1 and 2.2 for SEBS and TPU, respectively. Leading to an inability to sustain 100% elongation at room temperature. The blends of the different materials were chosen based on the tensile data that was previously gathered in this article. For the purpose of this demonstration, Table 2.4 shows the blends that were used to show the shape memory effect. After deformation, were able to calculate

R_f and R_r as will be seen later on. The specimen was elongated at room temperature to 100% elongation and then the load was released to record the ε_u value. The specimen was then heated at 80°C (the max tan δ temperature) in an oven for five minutes, removed, let to cool to room temperature, and then the ε_p value was recorded. The sequence of events is seen in the following Figures. The following figures illustrate the images for at least one of the specimens that were pulled for each blend that was chosen for a shape memory demonstration.

Figure 2.1 Delamination of PLA:SEBS tensile specimens at 45°.

Figure 2.2 Delamination of PLA:TPU tensile specimens at 45°.

Table 2.4 The number of specimens used for shape memory demonstration.

BLENDS	PLA/SEBS				PLA/TPU				Injecting Molding SEBS-TPU			
SHAPE MEMORY CHARACTERIZATION	X	X	X	3	2	2	2	2	X	X	2-3	2-3

Dynamic Mechanical Analysis (DMA) of the blend systems allowed for the determination of the glassy onset temperature as well as the max tan δ temperature. Our lab has found this data useful in the establishment of high temperature deformation and recovery temperatures for SMP materials. Illustrated in Figure 2.3 for PLA 4043D, if one were to deform a specimen at an elevated temperature, the glassy onset temperature could be used as the deformation temperature, while the original shape could be recovered by reheating the specimen to the max tan δ temperature. This figure is used as a reference/control for our material, where the deformation temperature is the temperature at which a material is deformed. While the recovery temperature is the temperature at

which a material recovers to its full original shape. Tables 2.5 and 2.6 indicate the values for the tensile control PLA data that will act as a reference for 3D printed and injection molding, respectively. Figure 2.4 illustrates three different tensile curves for 4043D PLA for 45°, 90° and injection molding. The PLA stress-strain curves will also be used as a control reference to compare with SEBS and TPU blends.

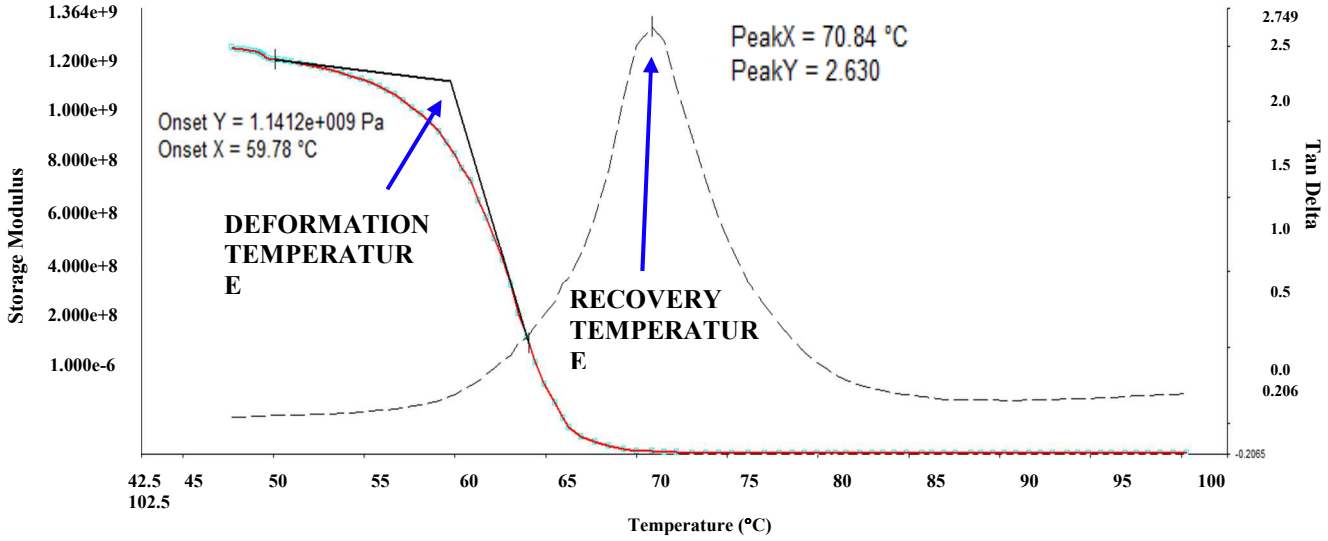

Figure 2.3 DMA spectra of pure PLA.

Table 2.5 Impact test values for 4043D PLA for 3D printed.

4043D PLA Izod Impact						
Impact Strength, J/m^2		Impact Resistance, J/m		Break Energy, J		Sample size (n)
AVG	STDEV	AVG	STDEV	AVG	STDEV	
4883	289	51	3.1	0.64	0.038	3

Table 2.6 Impact test values for 4043D PLA for Injection Molding.

4043D PLA Izod Impact						
Impact Strength, J/m^2		Impact Resistance, J/m		Break Energy, J		Sample size (n)
AVG	STDEV	AVG	STDEV	AVG	STDEV	
5093	139	54	1.4	0.68	0.019	3

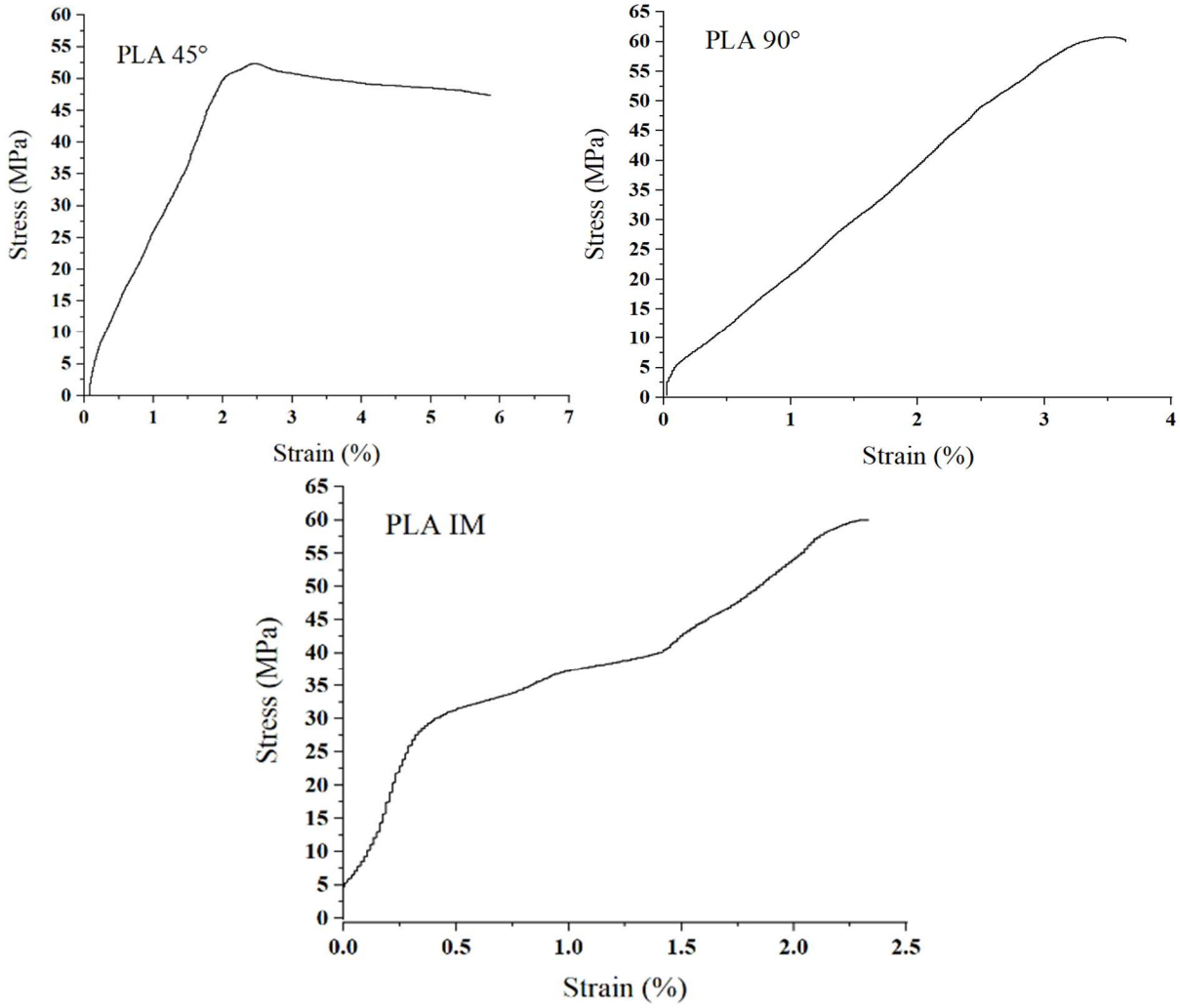

Figure 2.4 Stress-Strain curves for pure PLA 45°, 90° and injection molding.

Chapter 3

Results

In this chapter, we will be demonstrating the characterization analysis that was gather for the study of these two material blends. Illustrated in this study will be the dynamic mechanical analysis (DMA) of the 3D printed SEBS and TPU blends at different weight ratios. We will then demonstrate the x-ray diffraction (XRD) data that was obtained before undergoing thermal exposure and after thermal exposure and how the crystallinity of the material changes. Impact data using the Izod testing method will show the strength, resistance and break energy of the 3D printed and injection molding for both blends and all their different percentages. Fracture analysis will be determined using scanning electron microscopy (SEM) of the fracture surfaces of the impact specimens for 3D printed and injection molding materials. Finally, we will look at he tensile data that was obtained for all different raster patterns that were 3D printed and those that were injection molded. This will help determine which material blends will be used to test the shape memory effect of the blends.

3.1 DYNAMIC MECHANICAL ANALYSIS (DMA)

The DMA results for PLA:SEBS are numerically illustrated in Table 3.1.1 and their corresponding curves for the system are seen in Figure 3.1.1. Here it can be seen for 5% SEBS, 10% SEBS, 25% SEBS and 50% SEBS we obtained a tan δ of approximately 1.65, 1.54, 1.14 and 0.64, respectively. It is also noted that the temperature at which the maximum tan δ was recorded was the same (~80 °C) for all four blends. Three key observations can be made in this figure: 1) the window between max tan δ and glassy onset decreases with an increase in SEBS content (especially apparent when comparing with the curve for PLA in Figure 3.1.1); 2) the storage

modulus decreases with an increase in SEBS content; and 3) the max tan δ value decreases with an increase in SEBS content. The storage modulus for the PLA:SEBS system shows an increase in 10% and 50% SEBS, indicating elasticity of the material.

Table 3.1.1 DMA Spectra Results for PLA:SEBS.

Blends	*Tan Delta (Approx.)*	*Temperature (℃)*
PLA/SEBS 5%	**1.65**	**81°C**
PLA/SEBS 10%	**1.54**	**80°C**
PLA/SEBS 25%	**1.14**	**80°C**
PLA/SEBS 50%	**0.64**	**78°C**

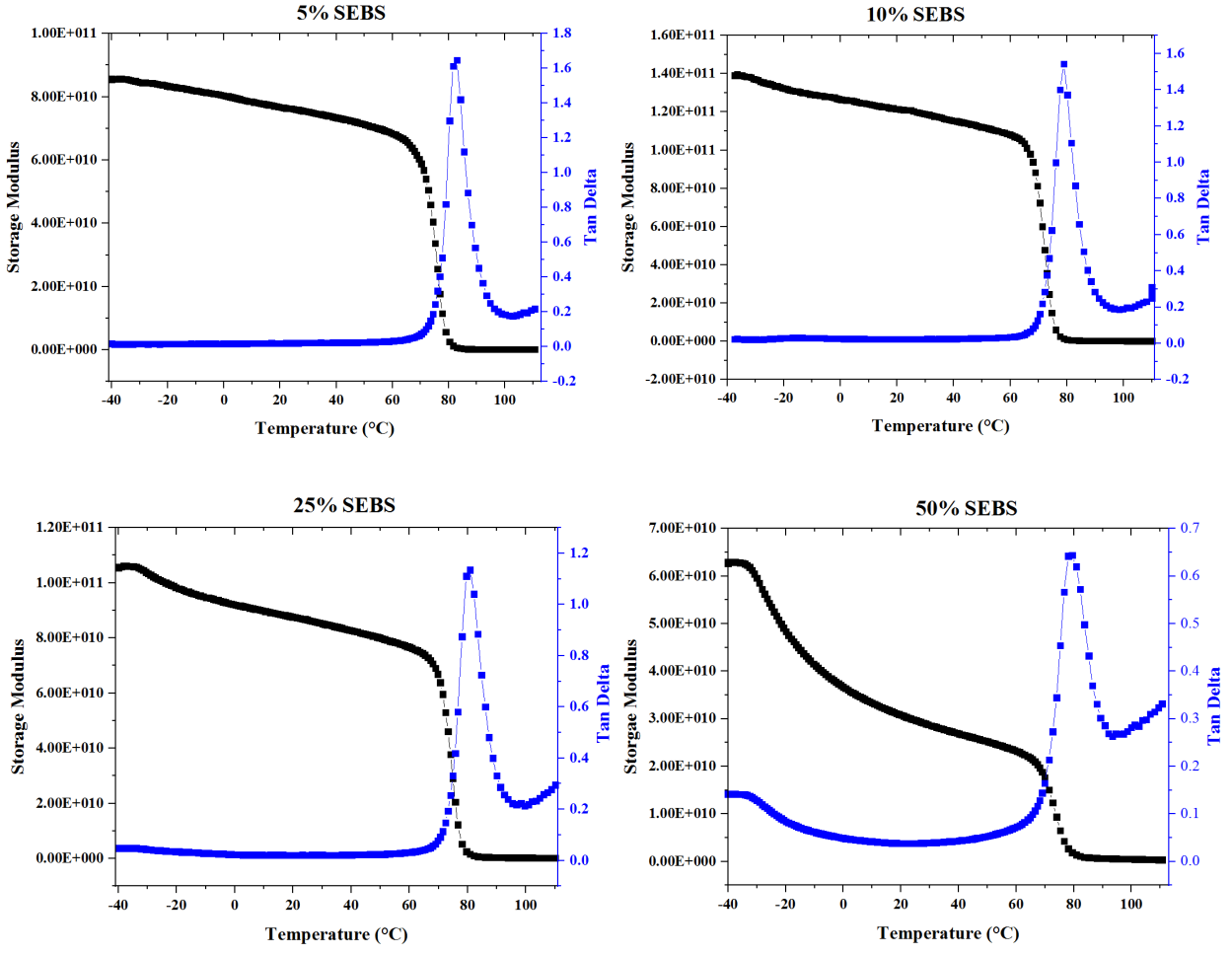

Figure 3.1.1 DMA Spectra for the PLA:SEBS blend system.

The DMA results for PLA:TPU are numerically illustrated in Table 3.1.2 and their corresponding curves for the system are shown in Figure 3.1.2. The information gathered shows that for PLA combined with by weight percentages of 5% TPU, 10% TPU, 25% TPU and 50% TPU we obtained maximum tan δ values of 1.51, 1.59, 1.35 and 0.55, respectively. There was a slight increase in tan δ for 10% TPU in comparison to other blends. Similar to the PLA:SEBS system with the same weight percentages, the temperature at which maximum tan δ was achieved was constant at around 80°C. It should also be noted that with increasing blend percentage, the tan delta approximation decreased for both material systems. An increase in storage modules is seen in the curves for 10% and 25% TPU, which gives rise to elasticity in a material.

Table 3.1.2 DMA Spectra Results for PLA:TPU.

Blends	***Tan Delta (Approx.)***	***Temperature (℃)***
PLA/TPU 5%	**1.51**	**77°C**
PLA/TPU 10%	**1.59**	**77°C**
PLA/TPU 25%	**1.35**	**77°C**
PLA/TPU 50%	**0.55**	**77°C**

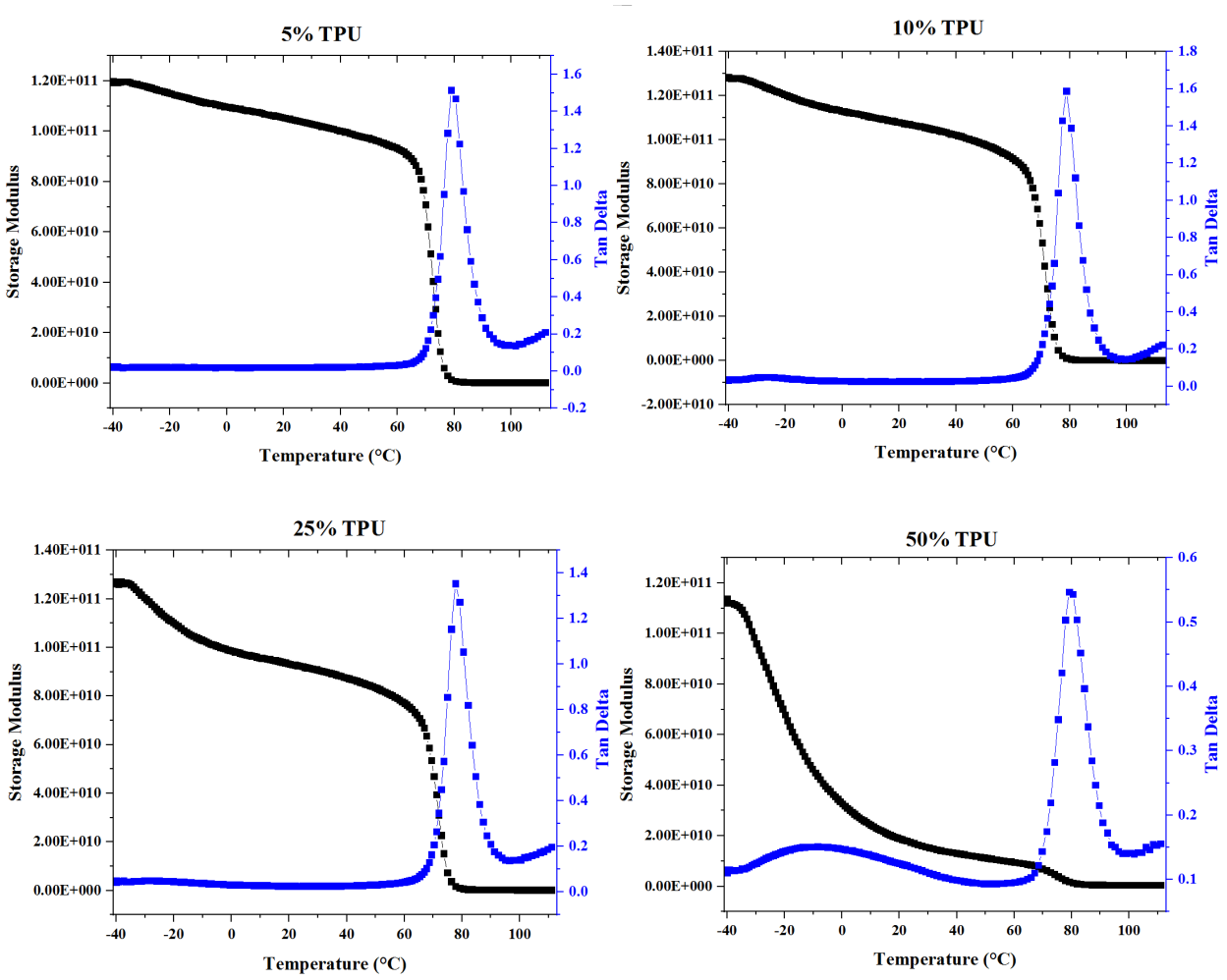

Figure 3.1.2 DMA Spectra for the PLA:TPU blend system.

3.2 X-RAY DIFFRACTION (XRD)

Analysis of the specimens via X-Ray diffraction (XRD) revealed that all blends composed of both PLA:SEBS and PLA:TPU compositions are amorphous in the as-printed state. XRD of these materials systems was considered due to their texture after undergoing DMA testing. Once the specimen was removed from the DMA chamber, most samples demonstrated to be flexible but with increasing blend percentage they became more rigid. In the figure below, there is a representation of the material property, which illustrated the amorphous region that is present roughly 20 degrees on the 2-theta scale. A noteworthy observation made in this study was that the

blend systems containing 5%, 25% and 50% SEBS and all blends for TPU rubber exhibited crystallinity after DMA testing as indicated by the peaks. PLA alone is known to be heat-treatable to the point of inducing crystallinity (Rocha Gutierrez, 2016). It is unclear as to why only the 10% SEBS blend was not crystallized by the DMA testing. The XRD spectrums are seen in Figure 3.2.1 and Figure 3.2.2.

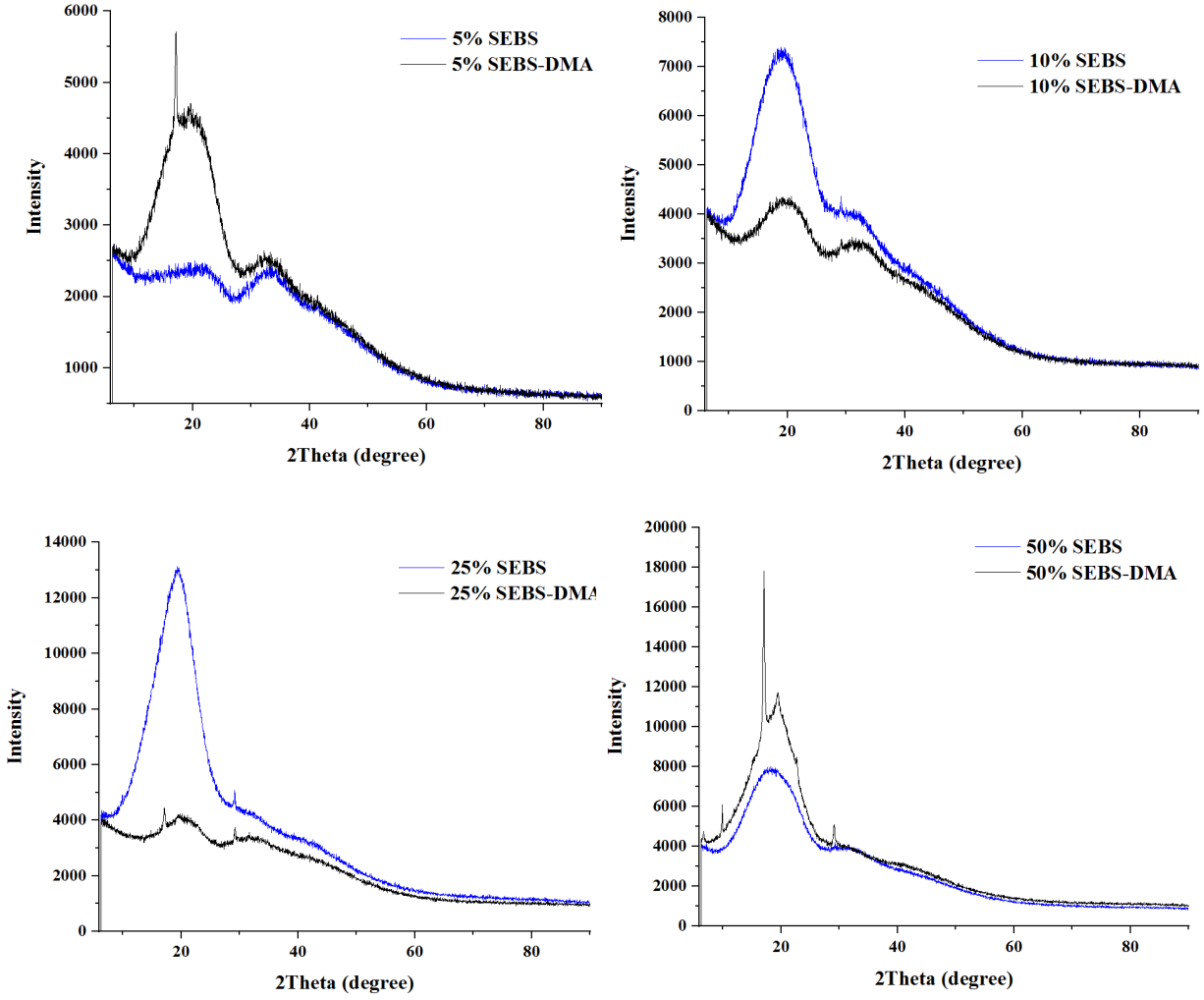

Figure 3.2.1 XRD Spectra for the PLA:SEBS blends.

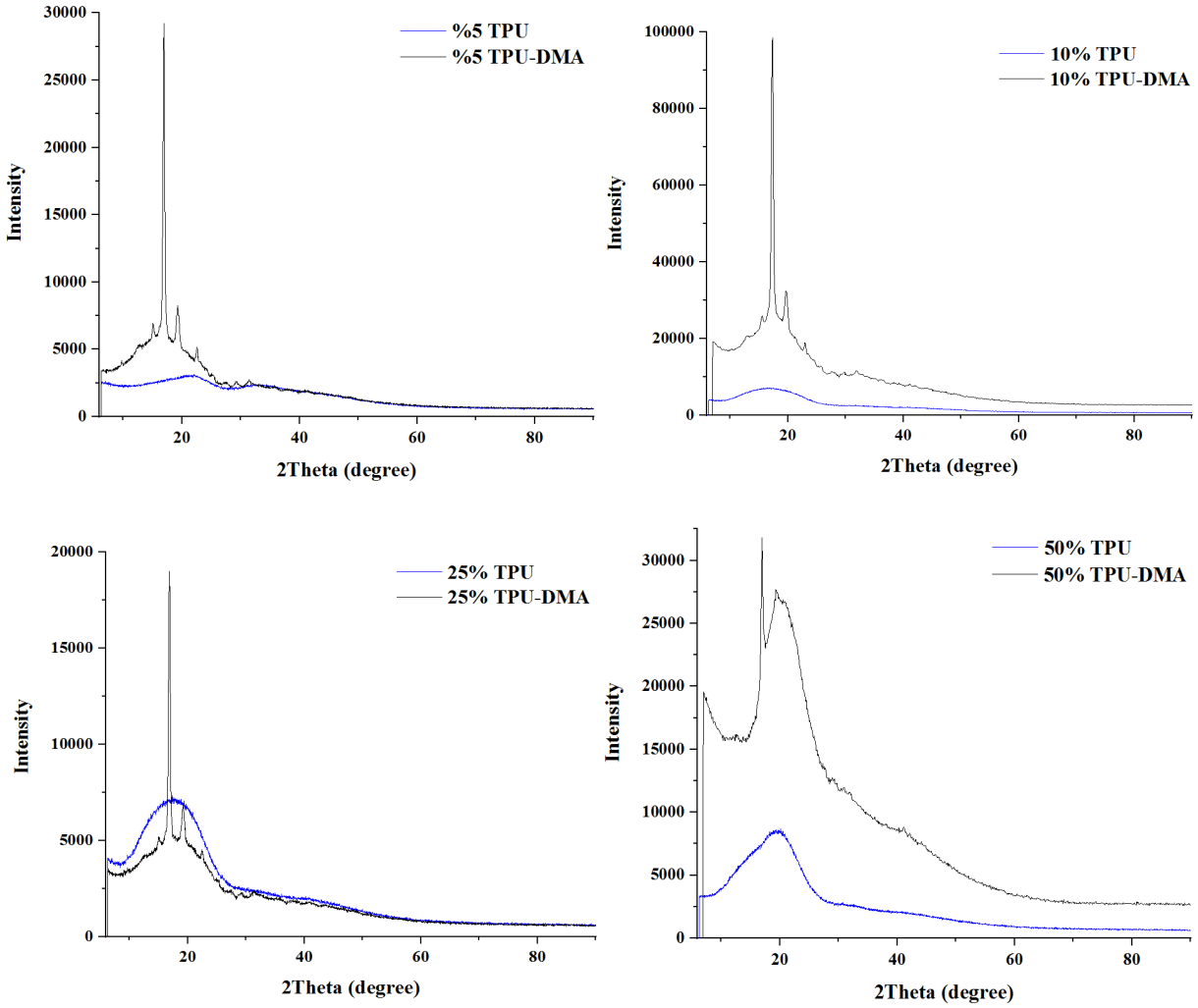

Figure 3.2.2 XRD Spectra for the PLA:TPU blends.

3.3 IZOD IMPACT TESTING

Impact testing of the PLA:SEBS showed a notable increase in impact strength of the material with an increase of weight ratio for this material system for the 25% and 50% PLA:SEBS blends. Table 3.3.1 is a representation of the impact values while, for brevity, we have plotted the impact strength in Figure 3.3.1. It is notable that none of the test specimens tested here totally ruptured due to the Izod impact test. All specimens were “hinged” after impact. This could be due to the presence of rubber in the material. Examples of this are exhibited in Figure 3.3.1. In

comparison to PLA:SEBS, PLA:TPU demonstrated higher values in strength, resistance and break energy. Table 3.3.2 shows that 50% TPU has the best overall results for all 3D printed specimens. This could be due to the rubber content for the material and that TPU is naturally more flexible than SEBS. Figure 3.3.2 shows the impact testing graphical demonstration of the 3D printed TPU specimens.

Table 3.3.1 Impact Test Values for SEBS% 3D Printed.

% SEBS	Impact Strength, J/m^2		Impact Resistance, J/m		Break Energy, J		Sample size (n)
	AVG	STDEV	AVG	STDEV	AVG	STDEV	
5%	4725	815	49	8.8	0.61	0.109	2
10%	4345	1145	45	11.8	0.57	0.148	2
25%	5853	3401	58	39.9	0.77	0.45	3
50%	19133	6451	201	67.6	2.53	0.843	3

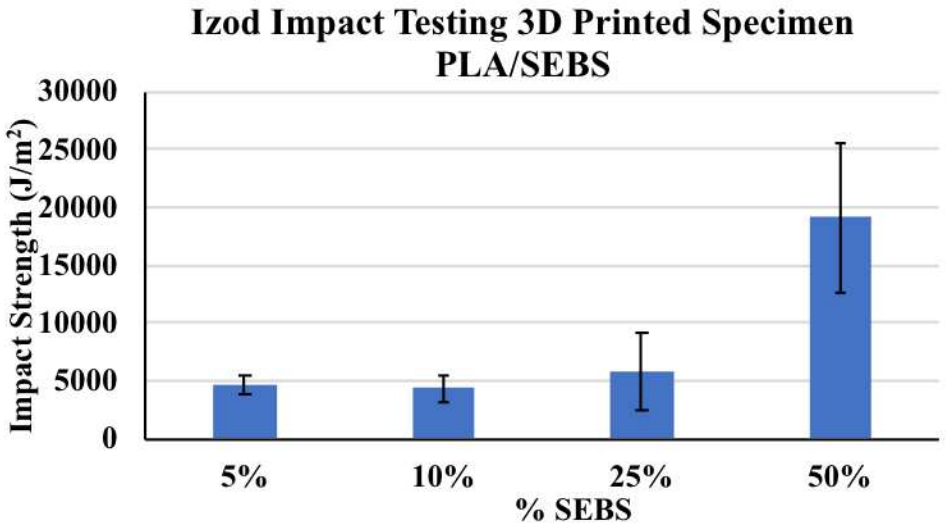

Figure 3.3.1 Impact strength of the 3D printed PLA:SEBS material system studied here.

Table 3.3.2 Impact Test Values for TPU% 3D Printed.

% TPU	Impact Strength, J/m^2		Impact Resistance, J/m		Break Energy, J		Sample size (n)
	AVG	STDEV	AVG	STDEV	AVG	STDEV	
5%	5630	73	58	0.9	0.73	0.009	3
10%	3287	1092	34	11.5	0.43	0.148	3
25%	9030	1180	95	13.12	1.18	0.17	3
50%	36167	1721	381	19.2	4.79	0.262	3

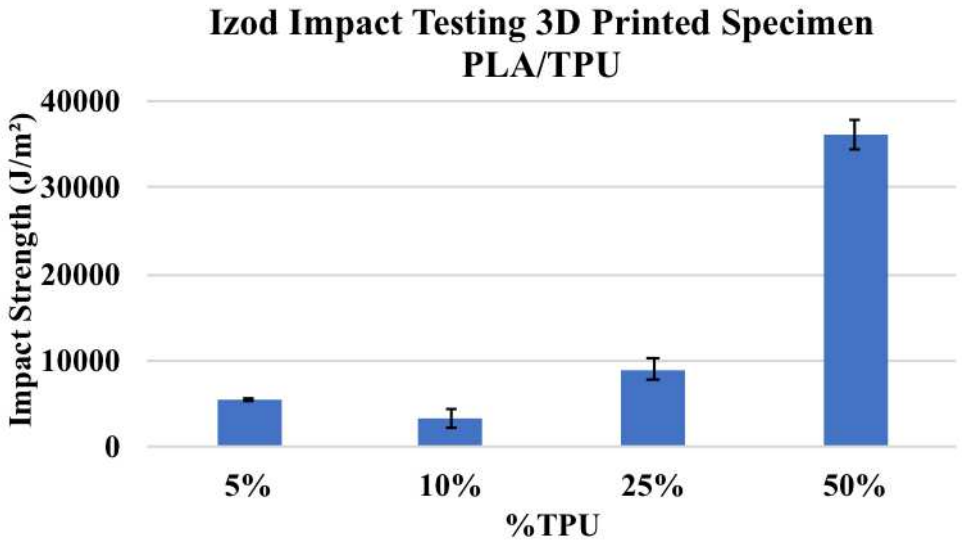

Figure 3.3.2 Impact strength of the 3D printed PLA:TPU material system studied here.

Impact testing of PLA:SEBS and PLA:TPU specimens fabricated via injection molding was also carried out.. In the case of injection molding the combination of PLA blended with 25% SEBS yielded the best results as compared to the other SEBS blends, as illustrated in Table 3.3.3 and Figure 3.3.3. In the case of PLA blended with TPU the 50:50 PLA:TPU composition yielded the greatest impact resistance values. Numerical data for the impact testing of the TPU blends is listed in Table 3.3.4 and graphically illustrated in Figure 3.3.4. The lower percentage blends had a full break for both materials, while 25% and 50% TPU did not fully break and exhibited "hinging" after the test was complete. The results indicated that 3D printed SEBS and TPU had a much higher overall strength resistance and break energy than injection molded specimens. This can be correlated with the fact that the injection molded specimens had defects such as those shown in

figure 3.3.5. PLA: TPU injection molding demonstrates a much higher strength than PLA:SEBS injection molding.

Table 3.3.3 Impact Test Values for SEBS% Injection Molding.

% SEBS	Impact Strength, J/m^2		Impact Resistance, J/m		Break Energy, J		Sample size (n)
	AVG	STDEV	AVG	STDEV	AVG	STDEV	
5%	3020	142	31	1.3	0.4	0.017	3
10%	3500	122	42.3	8	0.46	0.015	3
25%	5303	236	55.2	2.1	0.71	0.033	3
50%	3483	287	37.2	3.5	0.48	0.045	3

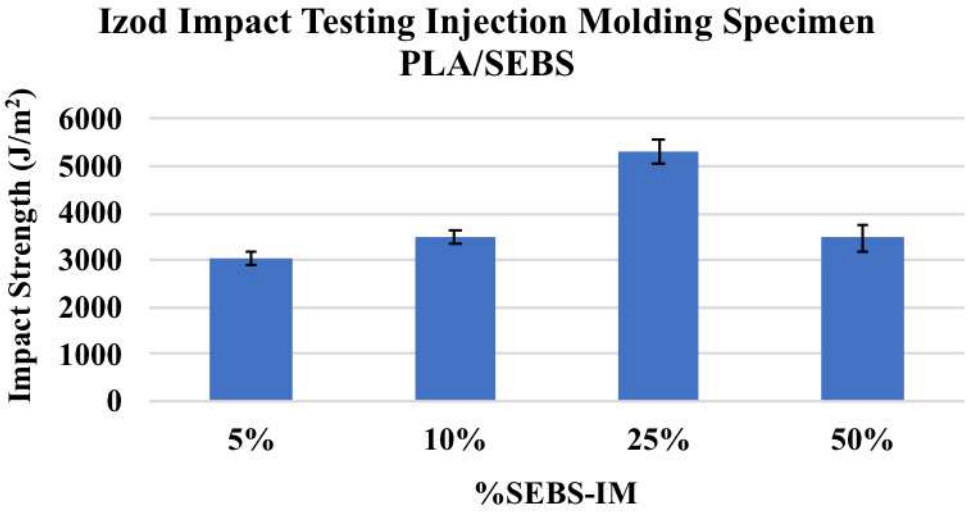

Figure 3.3.3 Impact strength of the injection molding PLA:SEBS material system studied here.

Table 3.3.4 Impact Test Values for TPU% Injection Molding.

% TPU	Impact Strength, J/m^2		Impact Resistance, J/m		Break Energy, J		Sample size (n)
	AVG	STDEV	AVG	STDEV	AVG	STDEV	
5%	2217	282	24	3.3	0.3	0.047	3
10%	2900	78	31	0.8	0.39	0.011	3
25%	3217	448	34	4.8	0.43	0.063	3
50%	13700	900	142	9	1.82	0.1	2

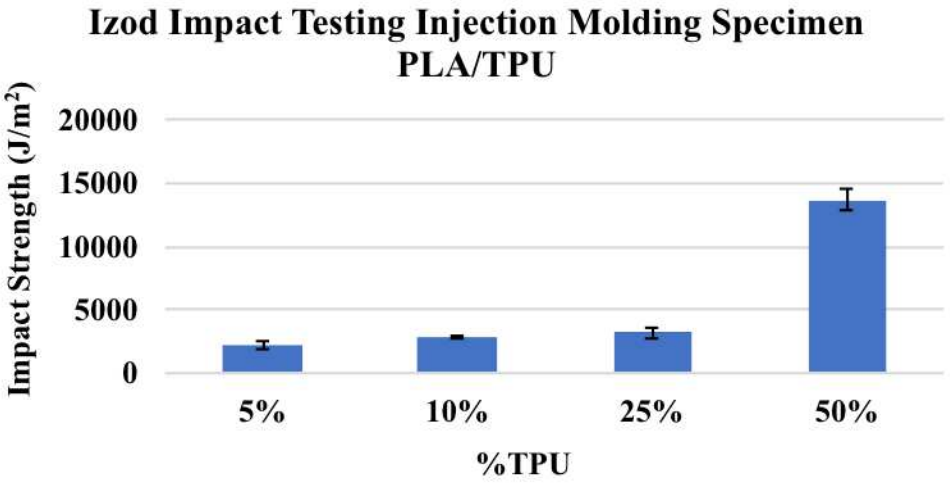

Figure 3.3.4 Impact strength of the injection molding PLA:TPU material system studied here.

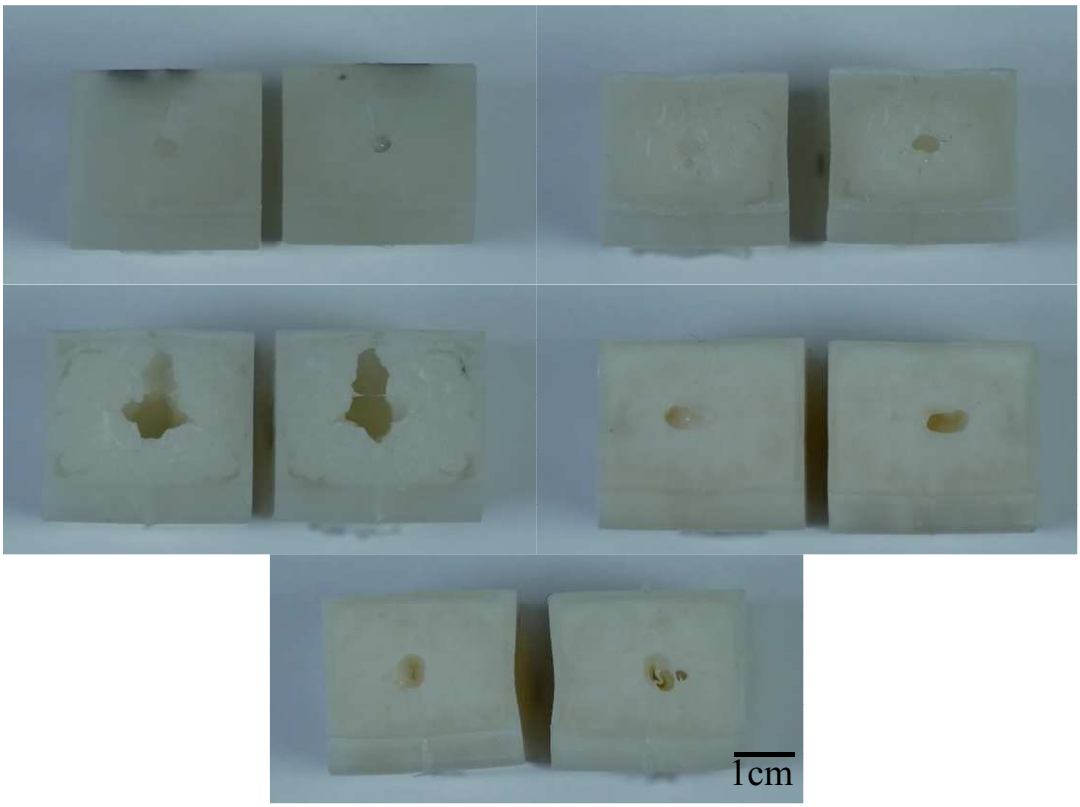

Figure 3.3.5 Images of injection molded SEBS and TPU specimens with voids.

3.4 FRACTURE SURFACE ANALYSIS

Scanning electron microscopy (SEM) microanalysis of the fracture surfaces of representative specimens from the PLA:SEBS blend system revealed that the fracture mode changes with an increase in SEBS content. All images were taken near the stress concentrator (V notch) of the specimens and taken at around 60x using backscatter electron detector (BSE), except for 10% that has a magnification of 30x and was taken using UVD. Starting with Figure 3.4.1a the fracture surface morphology is that of brittle mode failure. The steps on the surface are opened up craze cracks indicative of brittle failure (Perez et al., 2014). The fracture surface in Figure 3.5.1b is of the PLA:SEBS 90:10 blend. The higher rubber content has increased the ductility of the material and there is a greater amount of plastic deformation that has been seen in the micrograph of the PLA:SEBS 5:95 blend in Figure 3.4.1a. Both Figures 3.4.1c and 3.4.1d exhibit a greater amount of plastic deformation indicative of brittle mode failure where the bottleneck features in Figure 3.4.1d indicate necking of the individual print raster's occurred due to the impact testing. Large fibrils are highlighted by arrows in Figures 3.4.1c and 3.4.1d, which are also indicative of ductile rupture.

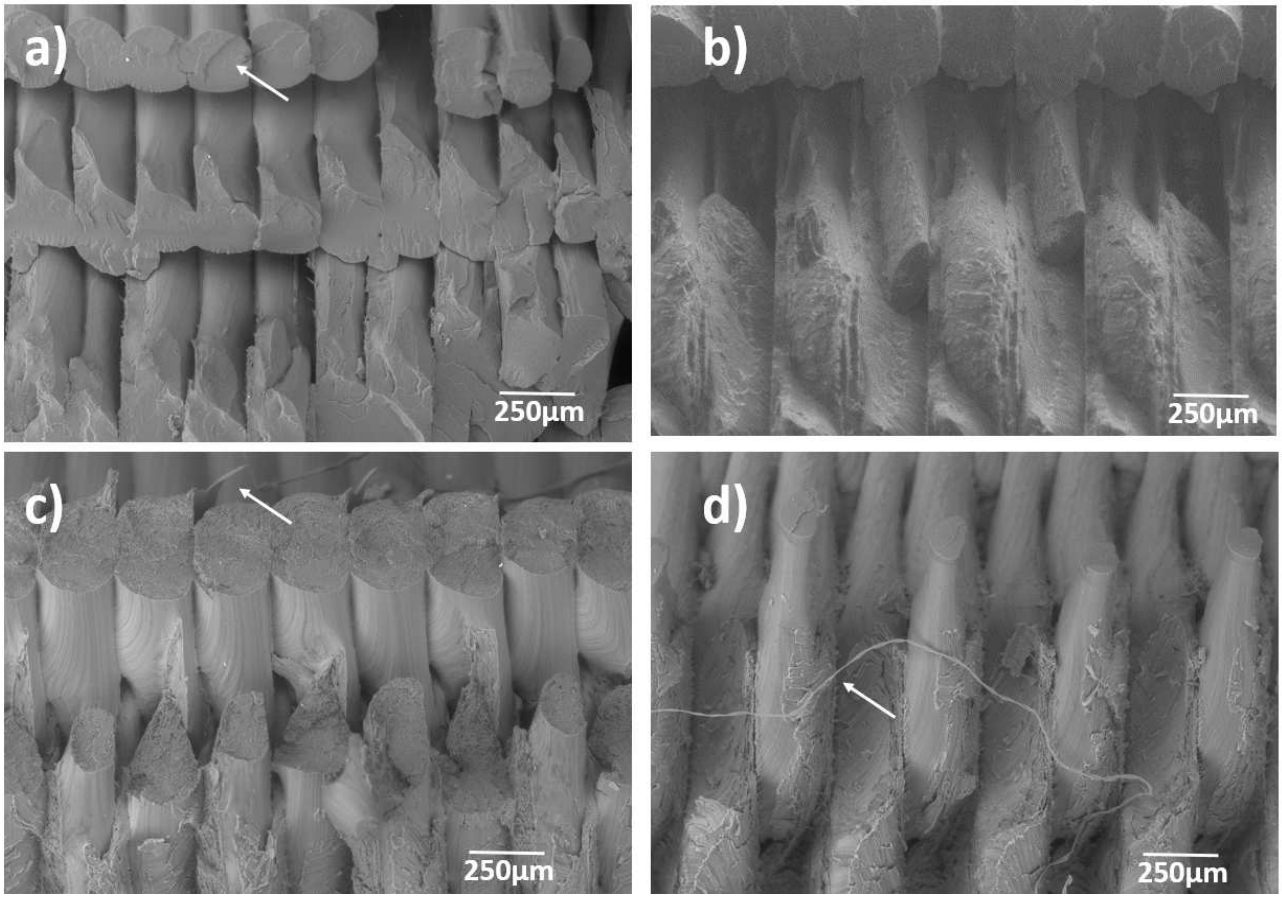

Figure 3.4.1 SEM Micrographs of impact test specimens for 3D printed PLA:SEBS where the compositions are as follows: a) 5%SEBS, b) 10% SEBS, c) 25% SEBS and d) 50% SEBS.

SEM images of PLA with TPU were also obtained to analyze the fracture surface of each blends after undergoing impact testing. The following images indicate that the fracture surface for this material changes drastically with increasing TPU percentage. All images of the PLA:TPU 3D printed system were taken at around 45x using BSE. Figure 3.4.2a shows plastic deformation at the surface and we can see a closer look at the bonding between 3D printed layers within the specimen. Comparing 3D printed SEBS to 3D printed TPU, fibrils are present much earlier in the material such as those seen in Figure 3.4.2b. An increase in plastic deformation is seen with increasing TPU percentage, as well as adhesion between layers that were 3D printing as shown in Figure 3.4.2c and 3.4.2d.

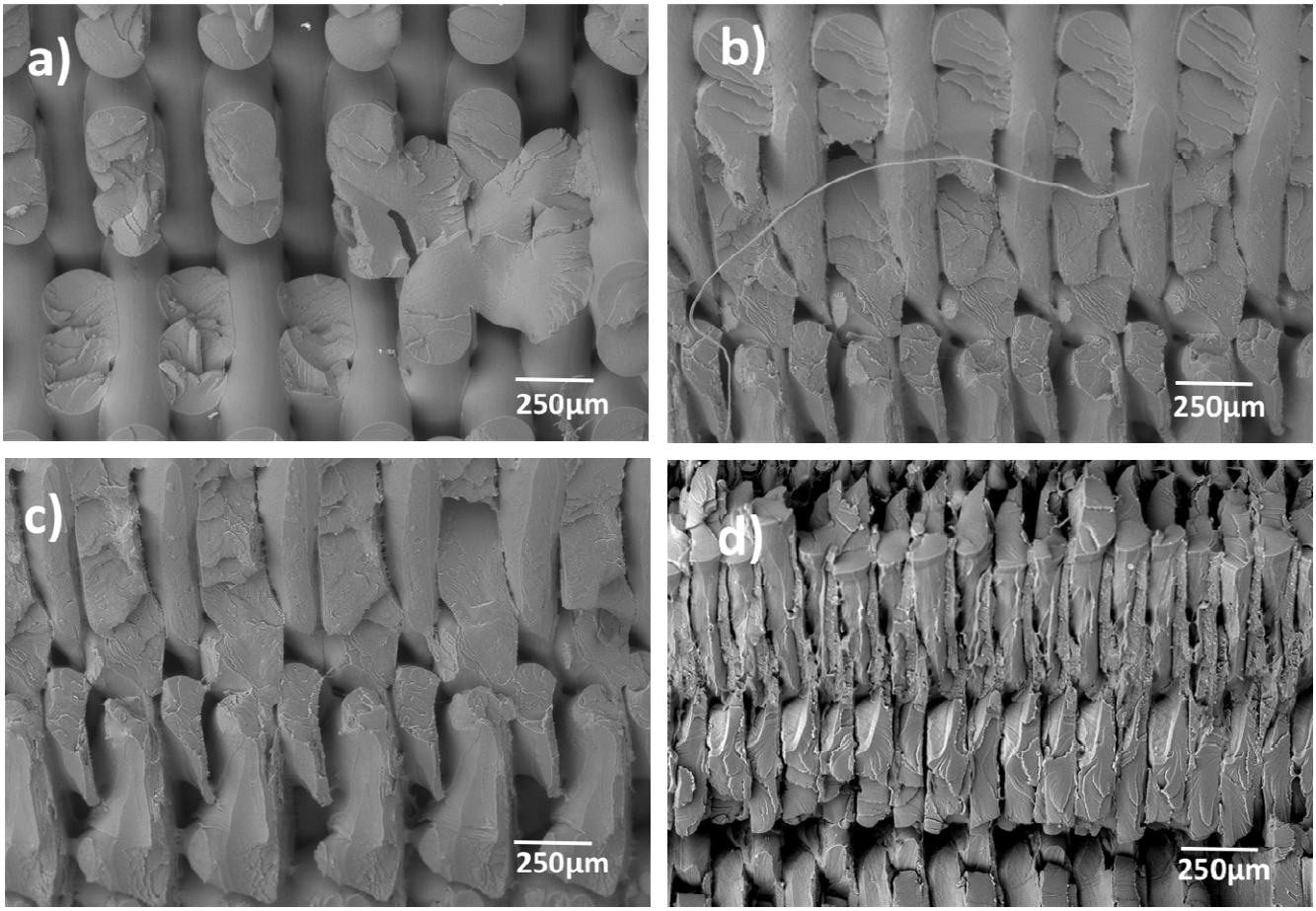

Figure 3.4.2 SEM Micrographs of impact test specimens for 3D printed PLA:TPU where the compositions are as follows: a) 5%TPU, b) 10% TPU, c) 25% TPU and d) 50% TPU.

Fracture surface analysis of injection molded SEBS impact specimens were also viewed under SEM to determine the fracture characteristics with increasing weight ratio. The images below for the PLA:SEBS system injection molding were taken at 35x for a and b using UVD and c and d were taken at 95x and 65x, respectively, using BSE. Figure 3.4.3a demonstrates a surge in fibrils and crack propagation. While Figure 3.4.3c and 3.4.3d reveal a non-uniform phase throughout both images, this indicates that polymer mixing between PLA and SEBS did not occur. The reason this is only observed on the injection molded fracture surfaces is that the features induced by the 3D printing process obscured any evidence of poor mixing. The fact that PLA and SEBS did not mix well agrees with the prediction made in Chapter 1 when the

miscibility parameters of the two materials was compared and found to be different. Figure 3.4.3d indicates fibrils and a greater amount of mixed brittle-ductile characteristics manifested during the impact test. An increase blend percentages exhibits more mixed mode brittle-ductile fracture surface features, while 5% SEBS showed a more uniform blend of both polymers. We can see a brittle-ductile-brittle surface, in which it is seen throughout all specimens analyzed under SEM for figures c and d, exhibited by immiscibility of PLA:SEBS.

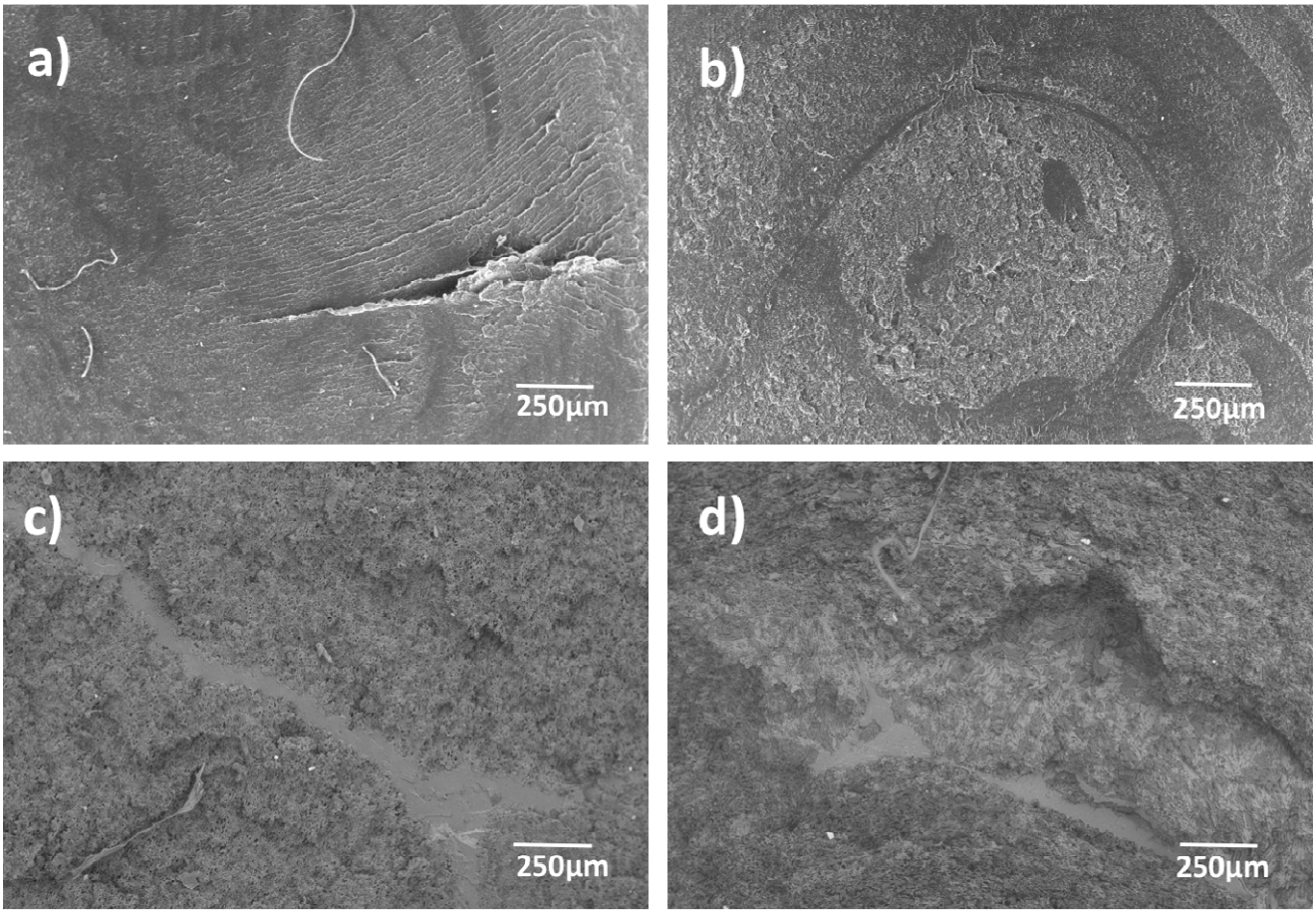

Figure 3.4.3 SEM Micrographs of impact test specimens for injection molding PLA:SEBS where the compositions are as follows: a) 5%SEBS, b) 10% SEBS, c) 25% SEBS and d) 50% SEBS.

Fracture analysis of the surface of injection molded TPU impact specimens are displayed in Figure 3.4.4. The images in the figure were taken 47x, 60x, 40x, and 70x for a, b, c and d, respectively, using UVD detector. All figures reveal striations within the polymer surface, an

increase in blend percentage shows a decrease in striations and a change in fracture mode. Where we can distinguish between to mode fractures in Figure 3.4.4d that show more clearly the break between a brittle mode to a ductile mode and striations.

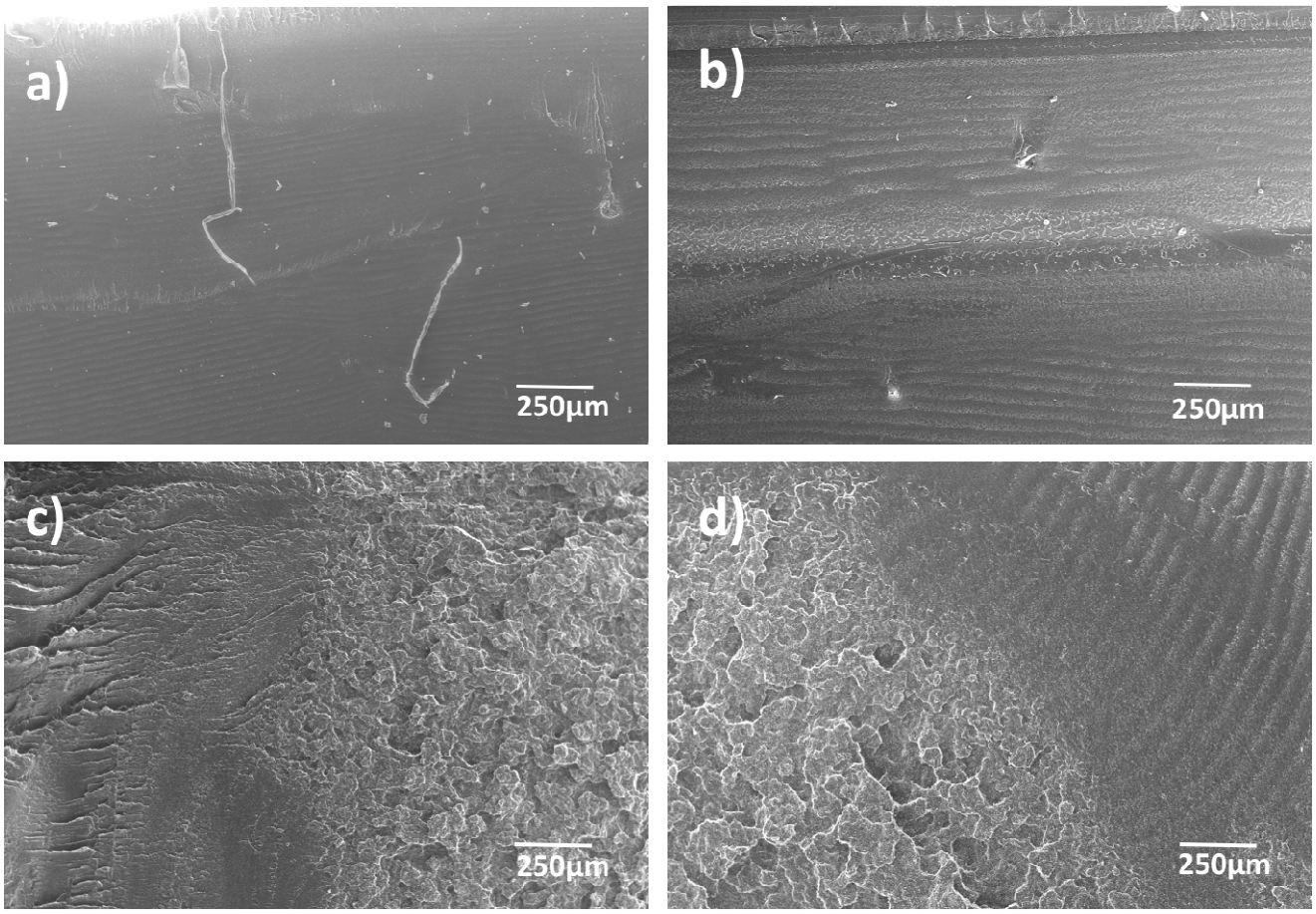

Figure 3.4.4 SEM Micrographs of impact test specimens for injection molding PLA:TPU where the compositions are as follows: a) 5%TPU, b) 10% TPU, c) 25% TPU and d) 50% TPU.

3.5 TENSILE TESTING

Tensile testing of the materials studied here was carried out to determine the tensile properties of the materials as well as to determine which material systems would be good candidates for the characterization of shape memory properties based on the % elongation values. The stress strain curves presented below are representative curves from each material compositions. Specimens fabricated in two raster patterns were compared with those fabricated

via injection molding. Tensile testing was done for pure PLA, SEBS and TPU and the resulting data was then used to determine the blend compositions that would be used for shape memory characterization based on the percent elongation being greater than 100%. As was explained in Chapter 2, specimens printed at 45° all failed or delaminated for both SEBS and TPU. The previously mentioned work performed by Chávez et al. (Chávez et al., 2018) compared three raster patterns and found that the longitudinal raster pattern exhibited both the best tensile properties as well as shape memory properties. As expected PLA did not exhibit a high amount of plastic deformation prior to failure and was only able to sustain percent elongation values lower than 10% for all manufacturing methods. It was also expected that adding either TPU or SEBS would constitute the rubber toughening of PLA, leading to greater % elongation values. In the case of blending PLA with SEBS, only the composition with weight percentages of 25% and 50% SEBS had the capability of straining to % elongation values greater than 100% making these blend combinations candidates for shape memory characterization. TPU had a higher strain overall than SEBS, we noticed that for injection molding only 25% and 50% were able to stretch enough to be used for demonstration, while longitudinal %TPU exhibits capabilities that would allow all blends to withstand 100% elongation. Longitudinal specimens at higher blend percentages showed delamination before reaching its failure point.

3.5.1 *Raster Pattern 45°*

Here, a comparison of the stress-strain curves for PLA:SEBS and PLA:TPU that were printed with a raster pattern of 45° is made by comparing the stress strain curves. The following figures below for the 45° rater pattern tensile specimens show the curves for the 3D printed SEBS and TPU blends. These curves show an increase in strain percentage with an increase of rubber

content. Delamination was a prevalent problem for specimens fabricated in this manner, and may be due to lack of optimized print parameters as well as the manifestation of stress concentrators due to print-related defects. This is seen in the section showing SEBS and TPU tensile specimen. While the composition of PLA:TPU 50:50 yielded strain values greater than 100% elongation, delamination still occurred and therefore, these specimens were not chosen for shape memory characterization.

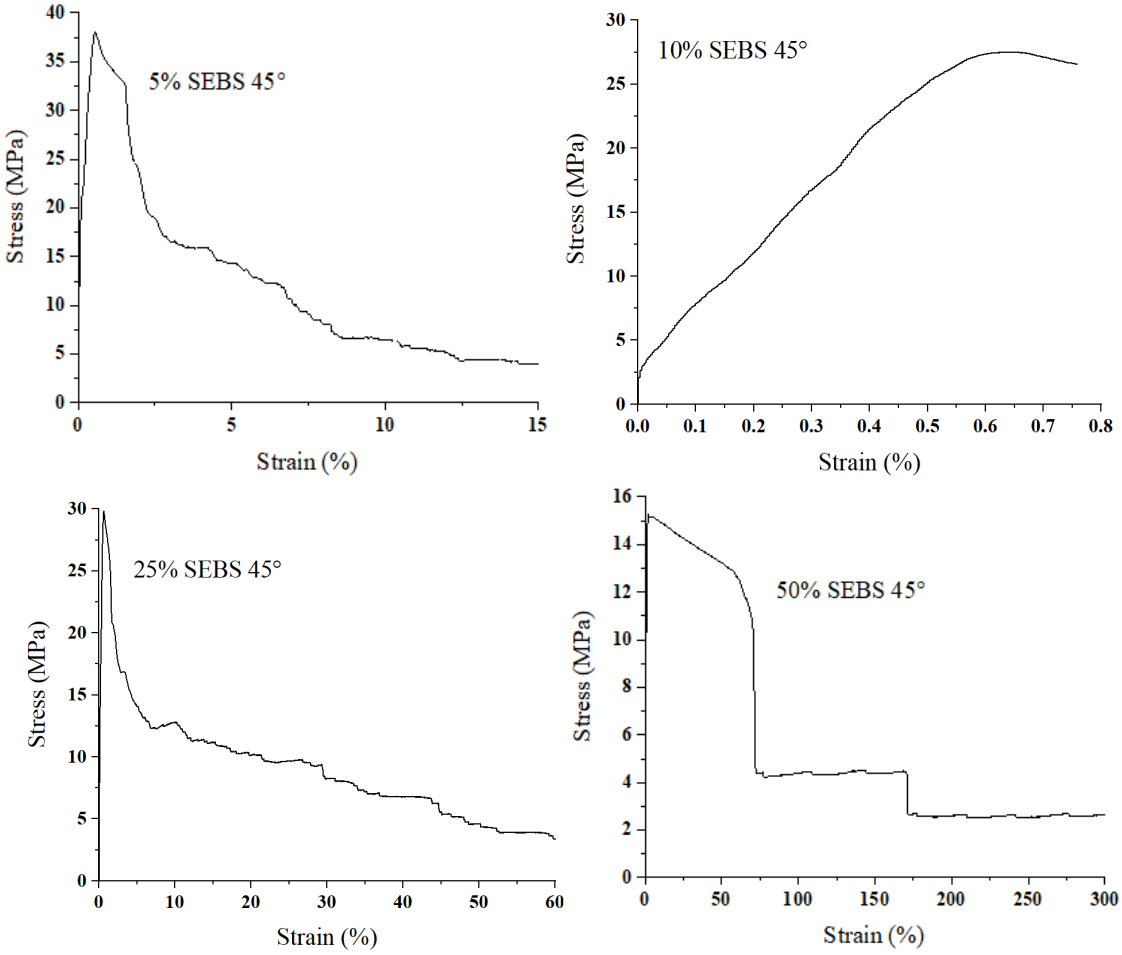

Figure 3.5.2 Stress-Strain curves for PLA:SEBS 45° raster pattern.

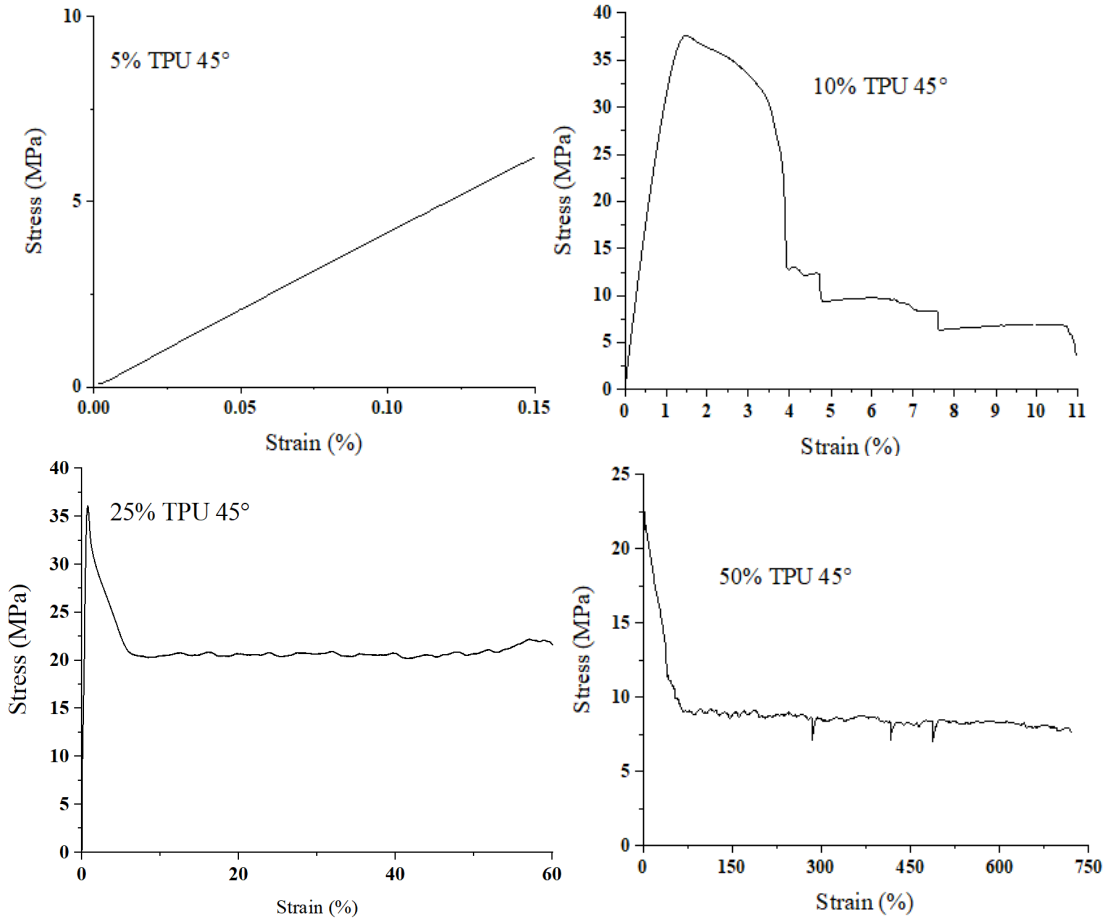

Figure 3.5.3 Stress-Strain curves for PLA:TPU 45° raster pattern.

3.5.2 *Raster Pattern 90°*

Comparing of the stress-strain curves for PLA:SEBS and PLA:TPU that were printed with a raster pattern of 90° allows us to determine the differences between the two rubbers as toughening agents for PLA. The curves clearly indicate an increase in strain percentage with increasing weigh percentage of elastomeric material. Because the print raster pattern is parallel to the applied load, higher stress and strain values overall compared to the 45° raster pattern. When comparing the two blend systems it is notable that SEBS blends have a much smaller strain values as compared to the blends of PLA and TPU. For example, the strain for 5% TPU reaches high percentages compared to any other blend within SEBS at 90° or even compared to 45°. The overall strain percentage for

TPU at 90° proves this specific combination of blends and raster pattern ideal for 100% elongation. This study indicated that all TPU blends will be good candidate for deformation at room temperature, while all SEBS blends showed a very low strain percentage which did not make them good candidates for the shape memory characterization given their inability to stretch to 25 mm without reaching failure.

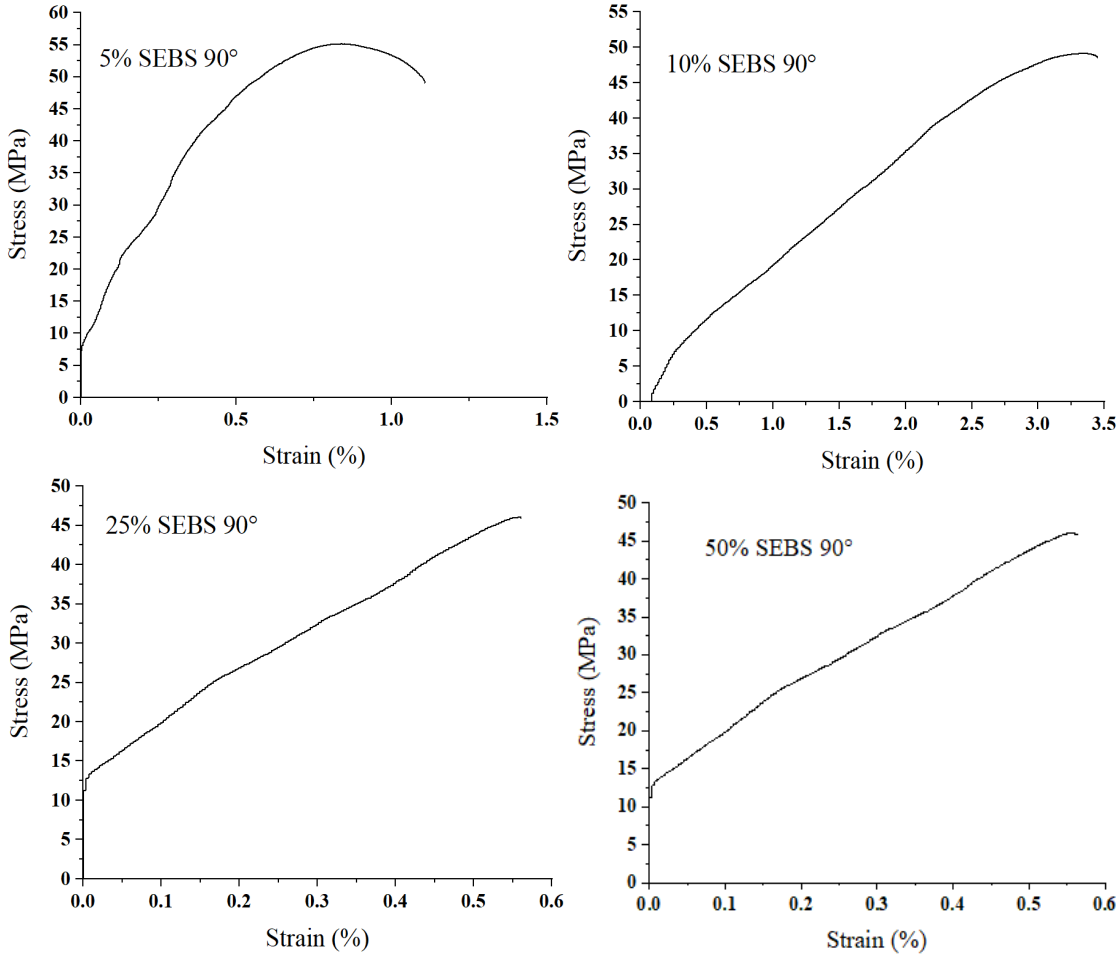

Figure 3.5.4 Stress-Strain curves for PLA:SEBS 90° raster pattern.

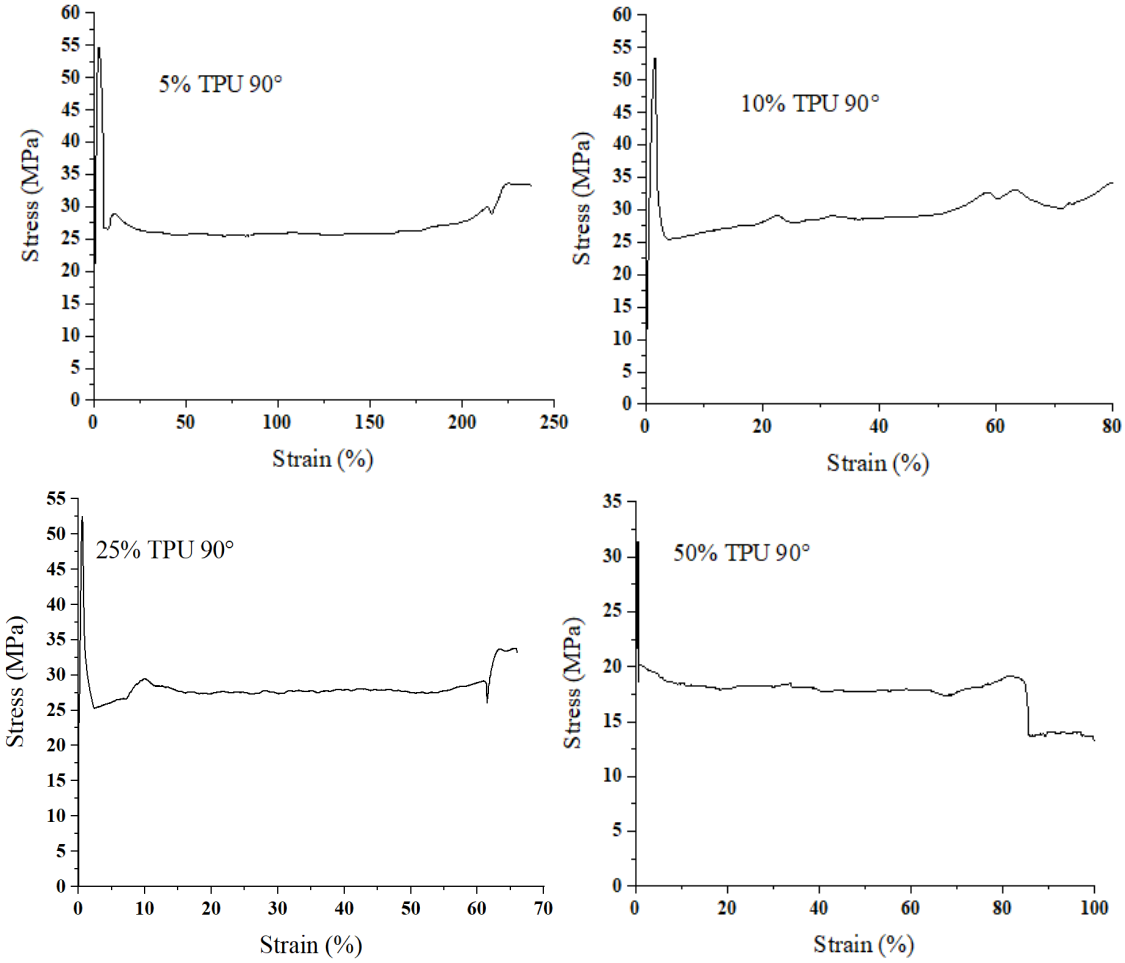

Figure 3.5.5 Stress-Strain curves for PLA:TPU 90° raster pattern.

3.5.3 *Injection Molding*

Here, a comparison of the stress-strain curves for PLA:SEBS and PLA:TPU that were injection molding specimens. These materials show similar behavior to the previous curves in different raster patterns, where the strain increases with blend percentage. The curves shown for injection molding with blends of 5% SEBS, 10% SEBS, 5% TPU and 10% TPU have a very small strain percentage that would not make them good candidates for deformation at room temperature. Making 50% SEBS, 25% TPU and 50% TPU the only valid candidate for a room temperature deformation.

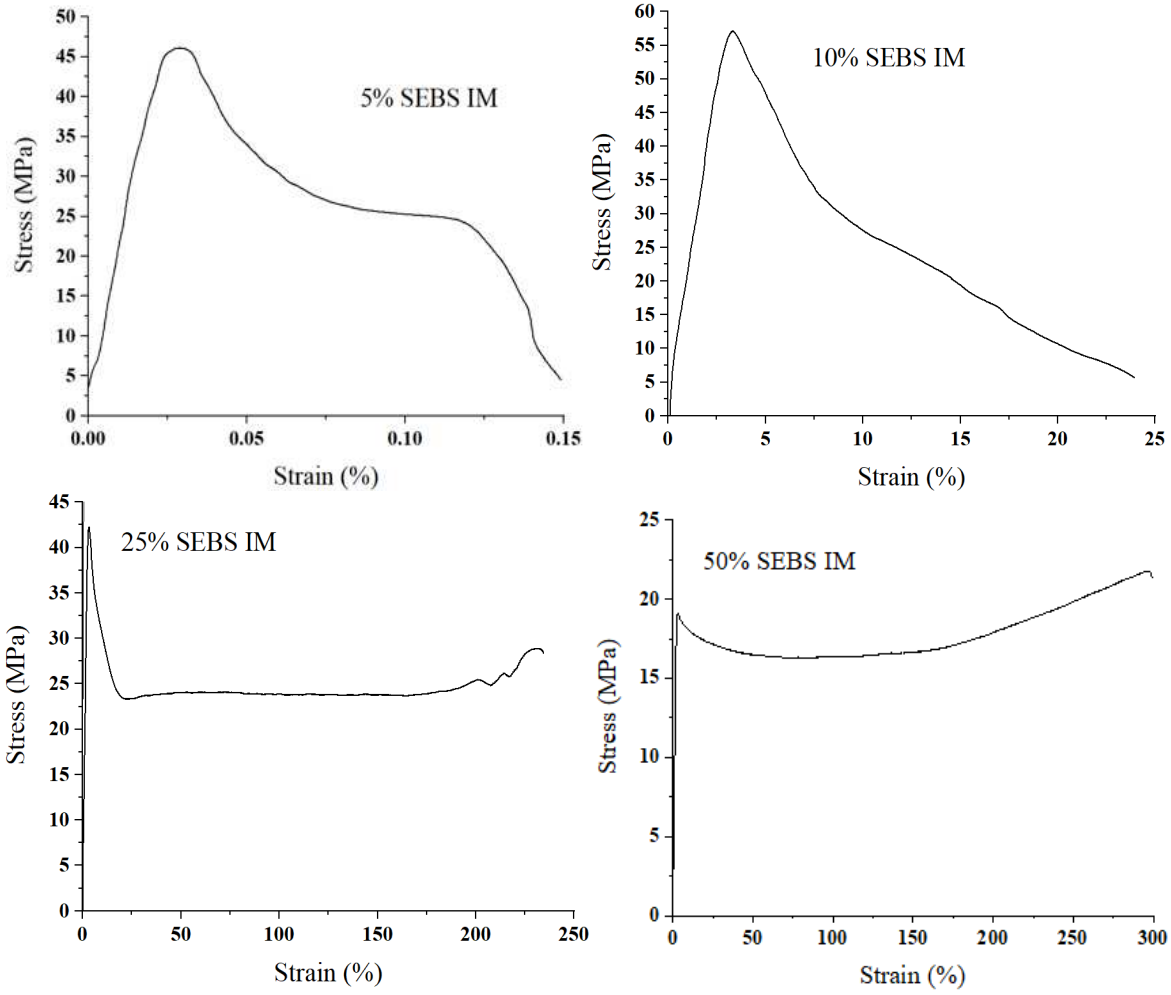

Figure 3.5.6 Stress-Strain curves for PLA:SEBS injection molding.

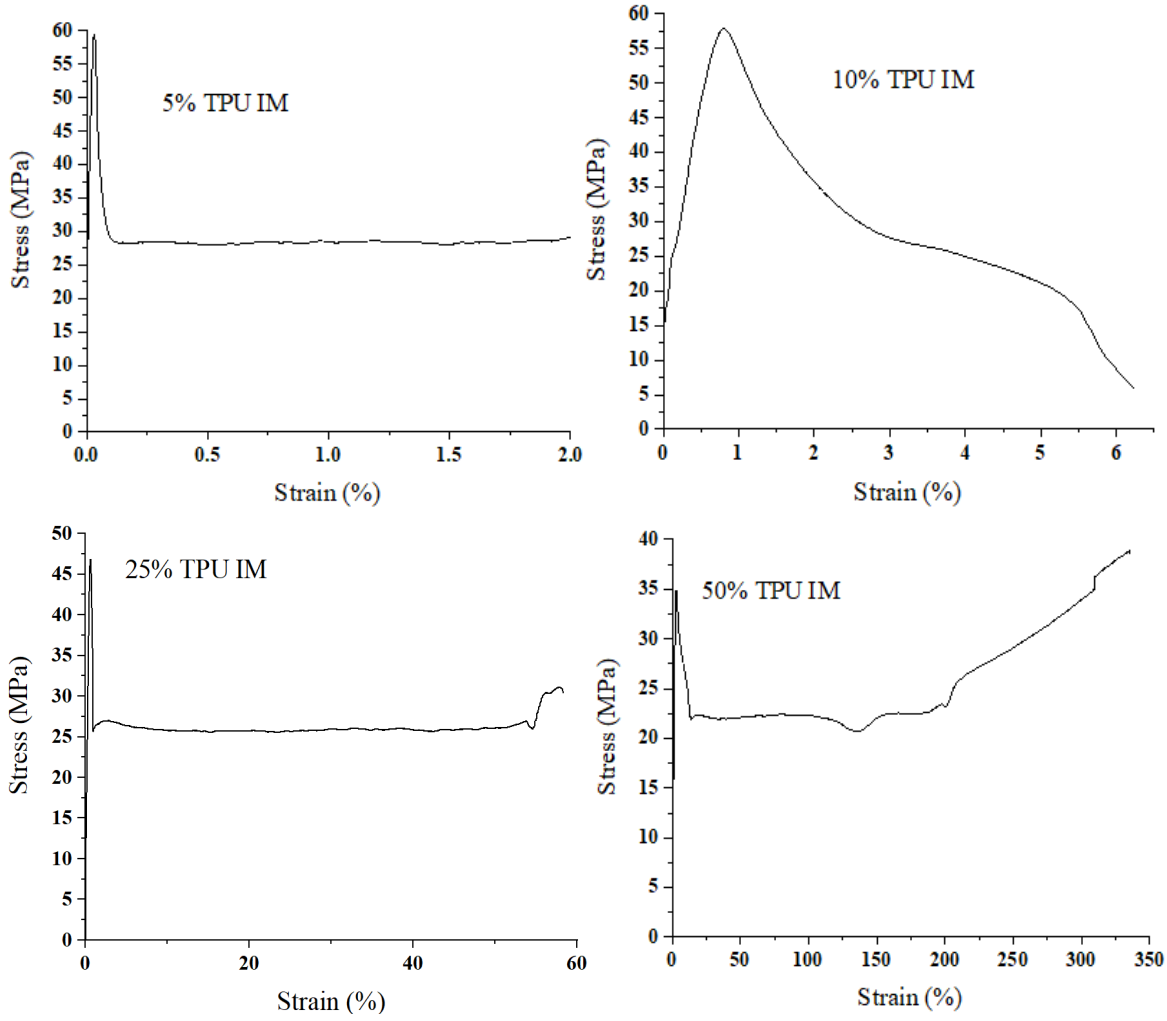

Figure 3.5.7 Stress-Strain curves for PLA:TPU injection molding.

3.6 SHAPE MEMORY CHARACTERIZATION

The shape memory characterization (SMC) is used to prove that by stretching a material to 100% elongation and heating to its recovery temperature it will regain nearly its original shape. Figure 3.6.1 illustrates the stress-strain curves of the blends in comparison to their raster patterns and injection molding. These were utilized to evaluate which specimens would be used for a shape memory characterization and if they would withstand to be stretch enough to reach elongation before failure. Although some stress-strain curves might demonstrate that 45° is a good match for

elongating 100%, this is due to delamination of the specimen and the high strain percentages are attributed to delamination of the raster patterns holding on to their perpendicular nature from the stress applied.

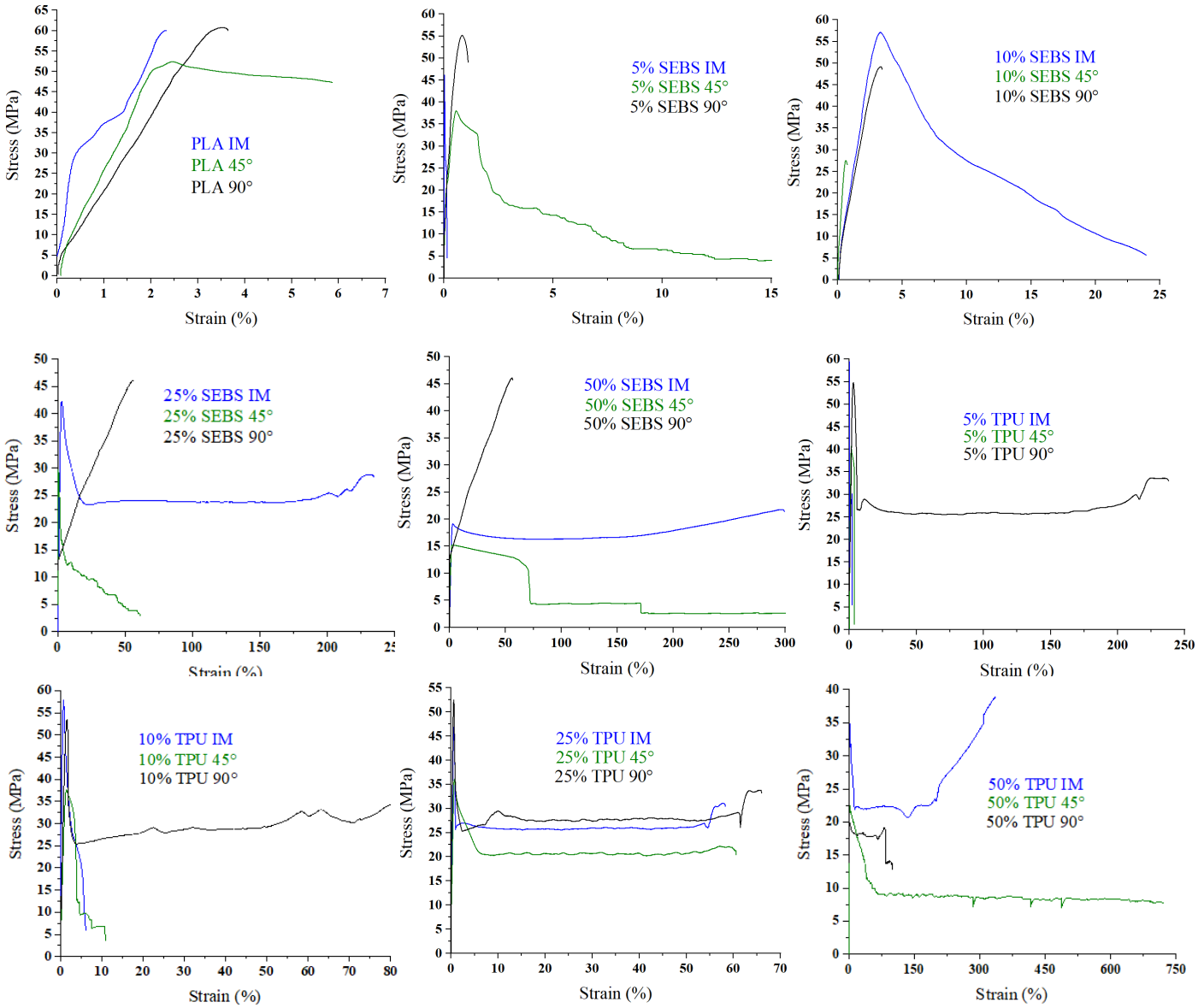

Figure 3.6.1 Graphical representation of tensile data in comparing each blend of PLA:SEBS and PLA:TPU to different raster patterns and injection molding.

Table 3.6.1 lists the values that were obtained for each specimen used for shape memory characterization. The key values of shape fixation, shape recovery and shape memory index are

tabulated. It is noteworthy that all specimens that were tested demonstrated a robust shape fixation as demonstrated by R_f values were nearly 95% or above with the lowest value being 94.8% even though the temperature of deformation was room temperature. The ability for the material to recover to its original shape upon subjecting the deformed specimens to heat. All materials demonstrated Rr values of 99%. The SMI values are all greater than 94% meaning that each material blend tested here behaves as a shape memory polymer as opposed to a rubber (Lai and Lan, 2013b). Even though most recovered nearly to their original shape, some still demonstrated some damage to the gage length after being stretched and recovered. The ability of specimens damaged by the deformation process to recover and effectively heal will be discussed in more detail below. As previously mentioned, all specimens fabricated with a 45° raster pattern were deemed incapable for use in shape memory characterization activities due to the inability to fully stretch specimens of any composition to 100% elongation at room temperature without delamination. Blends composed of PLA blended with 5% SEBS, 10% SEBS and 25% SEBS and printed with a 90° raster pattern as well as injection molded specimens of PLA combined with 5% SEBS, 10% SEBS, 25% SEBS, 5% TPU and 10% TPU were also discarded because fabricated specimens would rupture prior to attaining 100% elongation. The 50% SEBS printed with a 90° raster pattern was used as a demonstration of how a specimen recovers, even after undergoing partial failure. While the specimen was being stretched, it broke on one side as shown in figure 3.6.3. The elongation stopped recording but considering the material kept stretching on one side the test was continued. The specimen could not be stretched to 100% elongation within the gage length, therefore, no accurate calculation was able to be made for a fixation or recovery ratio. The deformation and recovery of 50% SEBS was technically unsuccessful due to no calculations, but it does show that even after partial failure, it can still recover what is left of the sample. This blend

demonstration can later be explored and help explain in more detail its properties and characteristics in shape memory polymers.

It should be noted that although injection molding 25% TPU shows results, it was stretched outside of the gage length and had to be modified to only calculate within the gage length which may result in inaccurate SMI % of the material. The extensometer for this material did not start calculating the 100% elongation until have way through the experiment due to stretching of the material happening outside the gage length. The crosshead was recording the data but then the extensometer started recording elongation within the gage length and we were able to calculate 100% elongation in the gage length. The issue with this is that the elongation is longer than what is really recorded and therefore, there is no accurate calculation of the stretching for this specimen but it was measured as if the gage length was the only stretching.

The highlighted row in Table 3.6.1 shows the highest fixation ratio and shape memory index of all the materials evaluated in this study, the combination of 50:50 PLA:TPU printed in the at 90° (longitudinal) raster pattern. It is speculated that this raster pattern outperformed injection molded specimens due to the alignment of phases due to the printing process as demonstrated by. It is notable that all materials selected for shape memory characterization demonstrated an excellent shape memory characteristic. The best overall material blend of 50% TPU at 90° can be compared in Table 3.6.1 to other blends.

Table 3.6.1 Critical shape memory properties for the materials systems selected for shape memory characterization.

BLENDS	ε_u	ε_p	R_f (%)	R_r (%)	SMI (%)
SEBS 50% (90°)-	CROSSHEAD				
SEBS 50% (IM)-I	49.76	25.34	99.52	99.99986	99.51986
SEBS 50% (IM)-III	47.41	25.42	94.82	99.99983	94.81984
TPU 50% (IM)-II	48.97	27.96	97.94	99.99882	97.93884
TPU 50% (IM)-III	47.4	27.66	94.8	99.99894	94.79899
TPU 5% (90°)-III	50.28	26.22	95.6621	99.99951	95.66163
TPU 5% (90°)-V	49.65	26.06	99.3	99.99958	99.29958
TPU 10% (90°)-I	50.35	26.57	97.88103	99.99937	97.88041
TPU 10% (90°)-III	49.58	26.56	99.16	99.99938	99.15938
TPU 25% (90°)-I	47.65	25.96	95.3	99.99962	95.29963
TPU 25% (90°)-II	49.3	26.2	98.6	99.99952	98.59953
TPU 50% (90°)-II	49.89	26.19	99.78	99.99952	99.77953
TPU 50% (90°)-III	49.45	27.02	98.9	99.99919	98.8992

Here, we will be explaining in greater detail each image of the different blends that underwent deformation during the shape memory demonstration. We will also be looking at the recovery of each blend and how well a material recovered or if there were any defects present to the specimen during the shape memory demonstration process. Photographic documentation of shape memory process where we deformed the specimens to a temporary shape at room temperature and then recovered the specimens in an oven allows for additional information pertaining to the ability of the materials to recover to be made. In the following figures there will only be one key image of each representative blend which were chosen based on features of their recovery. We also will take into considerations that were made to try each blend depending the stress-strain curves that were previously discussed and how these graphs serve as a guide for each specimen.

3.6.1 SHAPE MEMORY CHARACTERIZATION OF PLA:SEBS

The following images will illustrate the deformation each specimen underwent during the shape memory demonstration, the recovery and the defects (if any) that the specimens displayed after recover. Figure 3.6.2 give a step by step process of the shape memory demonstration (SMD) for 50% SEBS printed with a raster pattern of 90°. This particular blend demonstrated to have a strain percentage that was very low compared to other blends with different raster patters, but visually the specimen seems to have the capacity to stretch to 100% elongation. We believed it was worth testing for shape memory characterization to study its recovery with a defect. The following image illustrates that the specimen although was able to stretch, it split in the middle and broke on one side. We kept the specimen to see how it would recovery after it had partially reach failure, after placing the specimen in the oven at its tan delta temperature for recovery, we noticed even though the material shows delamination and failure it was still able to recover. Unfortunately, since the material failed the extensometer would not record its elongation so no actual calculations were able to be made for this specimen to not their fixation or recovery ratio. Figure 3.6.3 shows a closer look at the fracture surface of the specimen where it broken down the middle on one side and recovered on the other.

Figure 3.6.4 illustrates the shape memory demonstration for 50% SEBS injection molding, this specimen demonstrates to have recovered very well after undergoing deformation. No specific defects were noticed in this material after recovery. There is no evident defect in the material that would demonstrate that it had been stretched. Figure 3.6.5 illustrates a closer look at the recovered gage length, there seems to be no apparent defect left behind after recovery of the specimen.

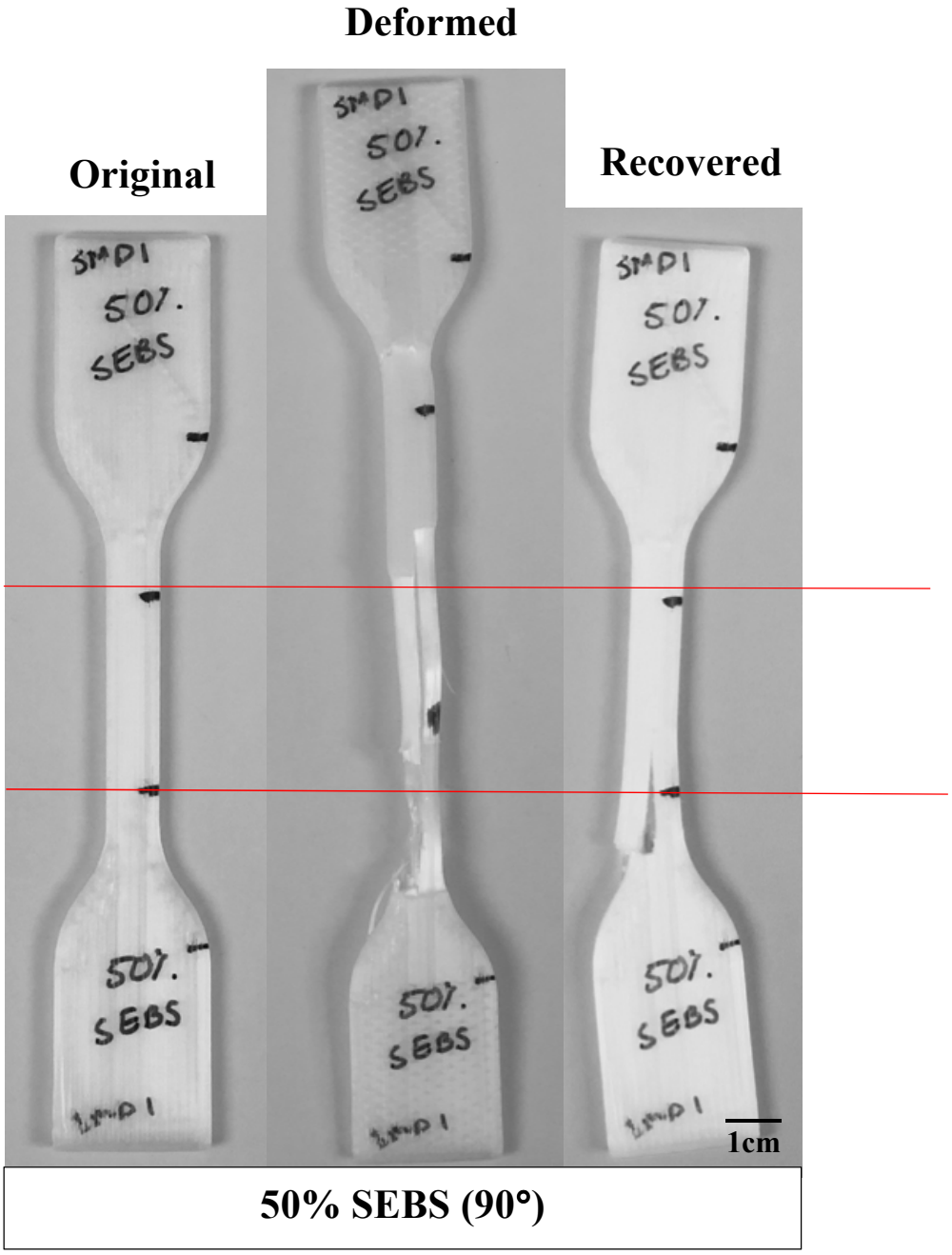

Figure 3.6.2 Photograph of 50% SEBS at 90° raster pattern where the specimen was stretched to 100% elongation and partly recovered at 80°C.

Figure 3.6.3 High mag. image of 50% SEBS at 90° raster pattern deformation after recovery.

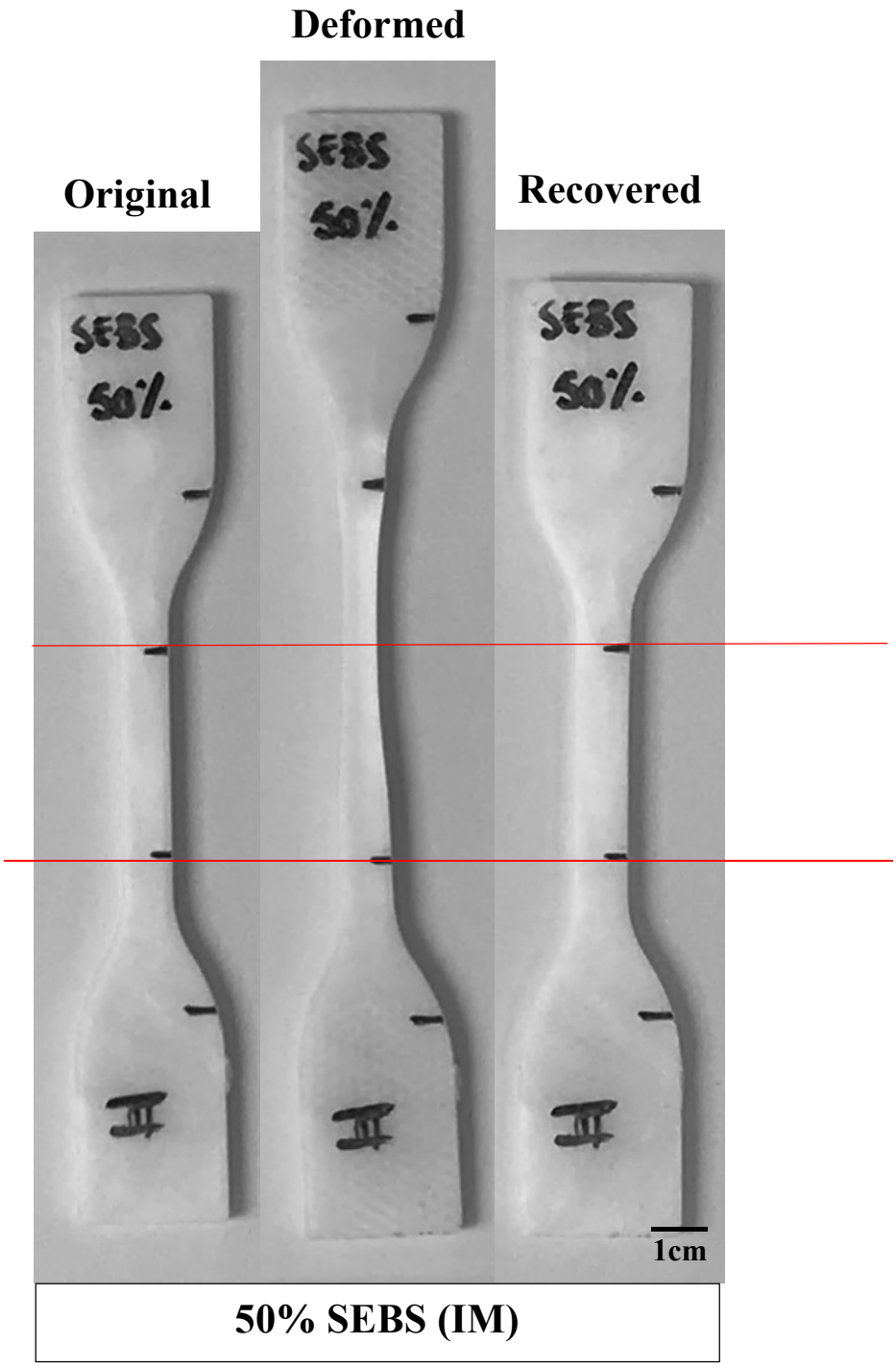

Figure 3.6.4 Photograph of 50% SEBS injection molding where the specimen was stretched to 100%elongationand partly recovered at 80°C.

Figure 3.6.5 High mag. image of 50% SEBS injection molding deformation after recovery.

3.6.2 SHAPE MEMORY CHARACTERIZATION OF PLA:TPU

Presented here is the deformation each specimen underwent during the shape memory demonstration, the recovery and the defects (if any) that the specimens displayed after recover. Figure 3.6.6 shows the SMD for 50% TPU injection molding where we can see that while the specimen was successfully stretched to the intend elongation, the recovery demonstrated a defect on the side and back of the specimen. It also let the specimen crooked due to the defect after recovery. The next demonstration illustrates 5% TPU stretched and recovered, although it is hard to distinguish, 5% TPU after recovery shows a line on the surface of the specimen due to stretching. Figure 3.6.8 shows only the deformation and recovery images of 5% TPU due to human error in which no image was taken before the specimen underwent deformation. There is no dominate defect present, but we can see some strain whitening in the gage length that could be due to the stretching of the specimen as illustrated in Figure 3.6.9. The following image illustrates 10% TPU in Figure 3.6.10, here we can see the sample before deformation, the deformation and the recovery images of the specimen. This blend shows bumps on the surface of the gage length after recovery, in which we can see that are present in two different spot that seem to illustrate exactly were the specimen was stretched. The defects are indicated by the arrows shown in Figure 3.6.11. The small bumps defects presented on the surface seem to also be the cause for the specimen to be left crooked, meaning that on the inside there might still be some grater deformation. Figure 3.6.12 shows the SMD for 25% TPU and it is clearly observed the immediately after the deformation, the specimen was crooked. The specimen was successful in recovery nearly to its original shape but there were some apparent defects on the surface of the gage length. The defects after recovery can be seen in Figure 3.6.13 and are indicated by the arrows at different perspectives of the sample, there are three defects illustrated in the middle on the surface of the gage length. The specimen

demonstrated defects such as lines and crooked specimen after the recovery was documented. Finally, Figure 3.6.14 gives light to the SMC of 50% TPU where the gauge stretched with no delamination or out of plane deformation. No defects were observed after recovery and it was the best performing material in terms of shape memory properties. The specimen appears to have strain whitening in the middle of the gage length due to stretching and recovery of the sample. A closer look at the gage length of the material can be seen in Figure 3.6.15 where the arrow indicated the region of the strain whitening.

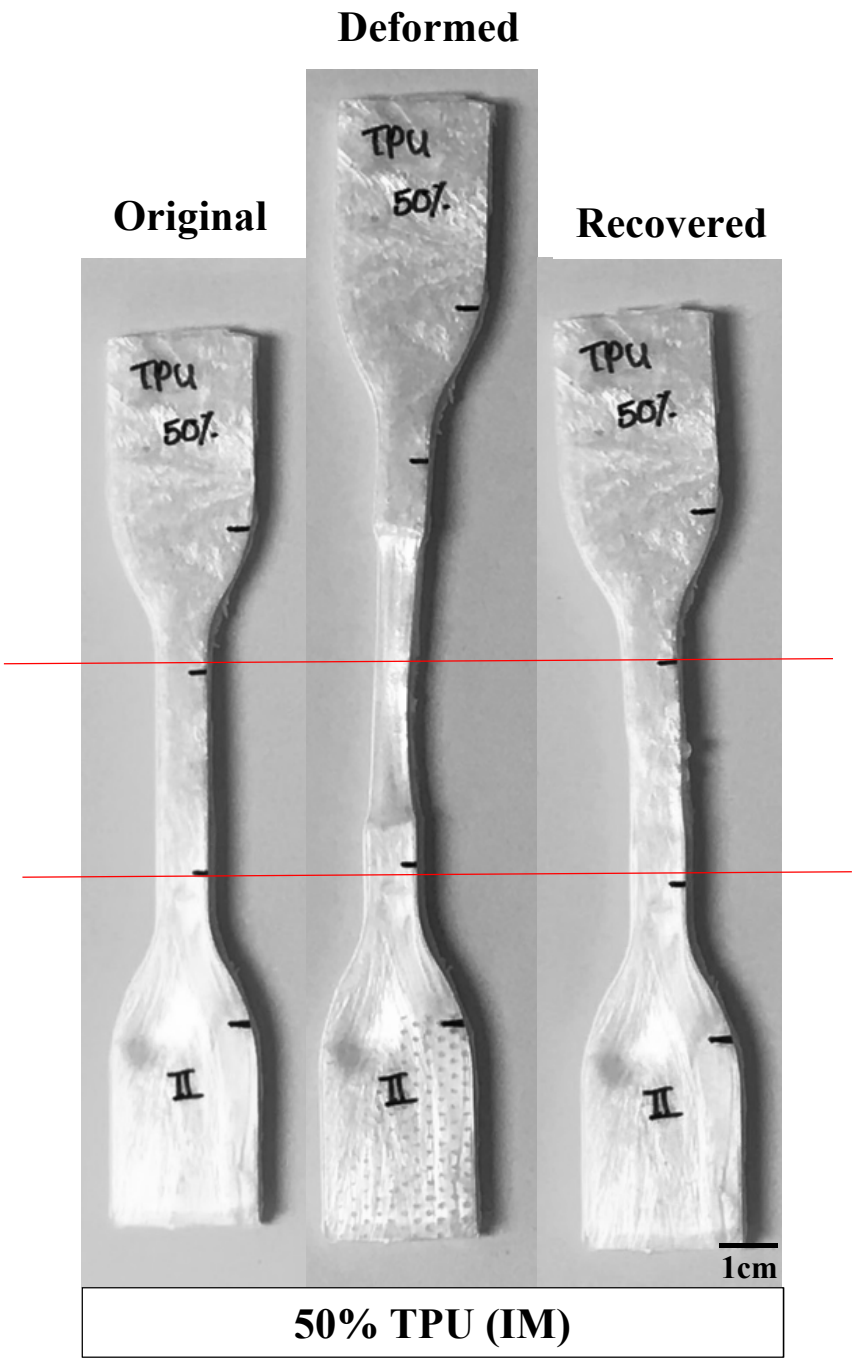

Figure 3.6.6 Photograph of 50% TPU injection molding where the specimen was stretched to 100% elongation and partly recovered at 80°C.

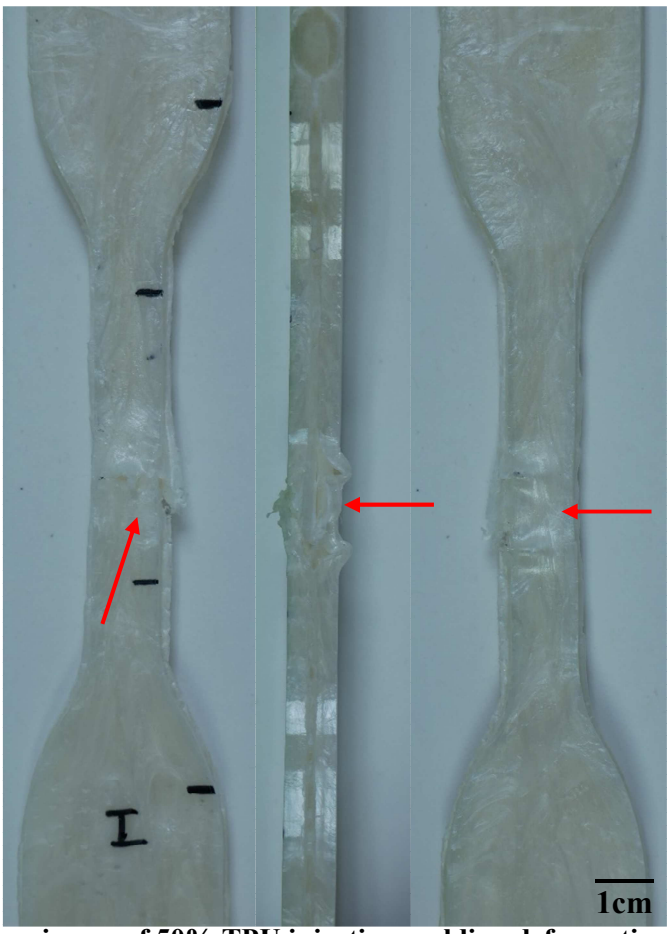

Figure 3.6.7 High mag. image of 50% TPU injection molding deformation after recovery.

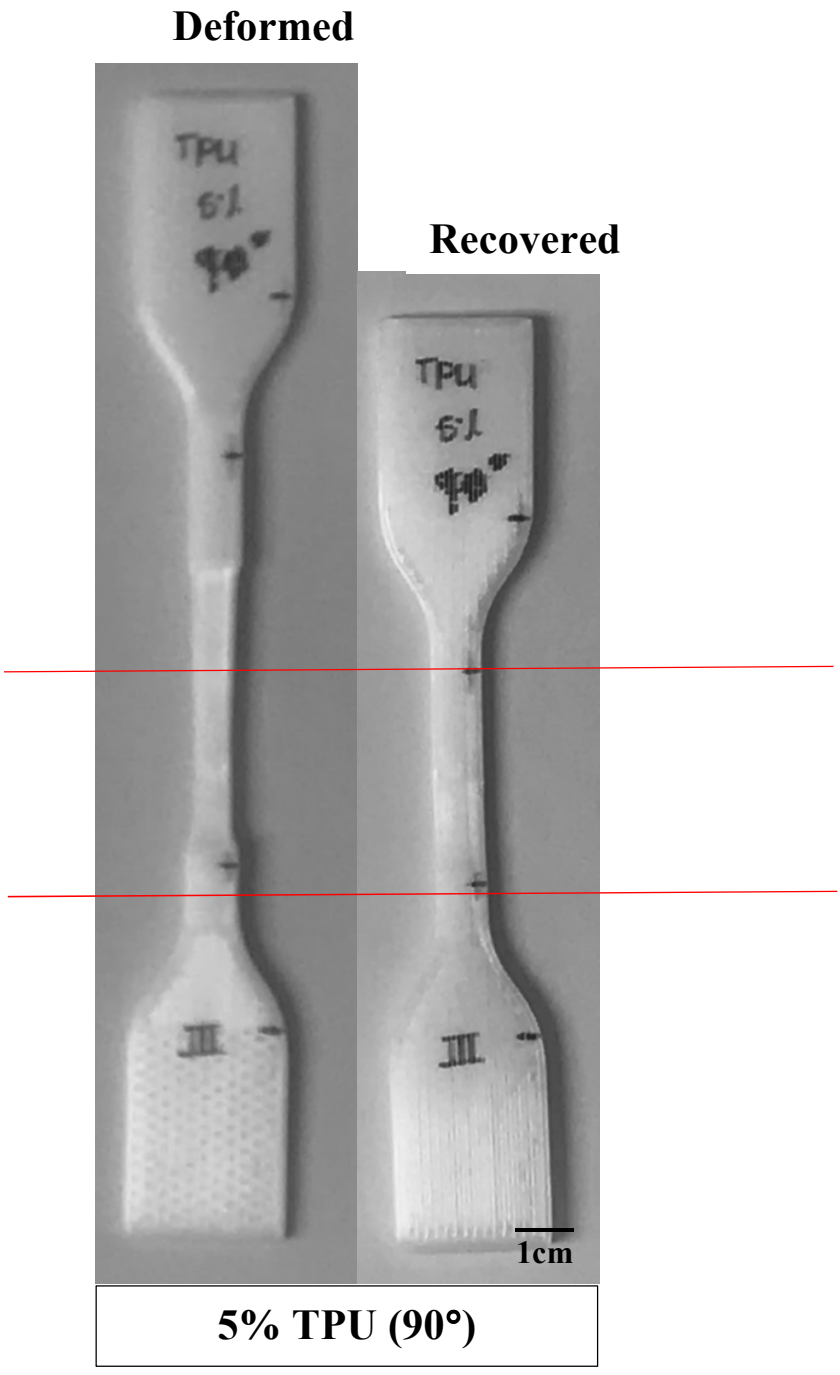

Figure 3.6.8 Photograph of 5% TPU at 90° raster pattern where the specimen was stretched to 100% elongation and partly recovered at 80°C.

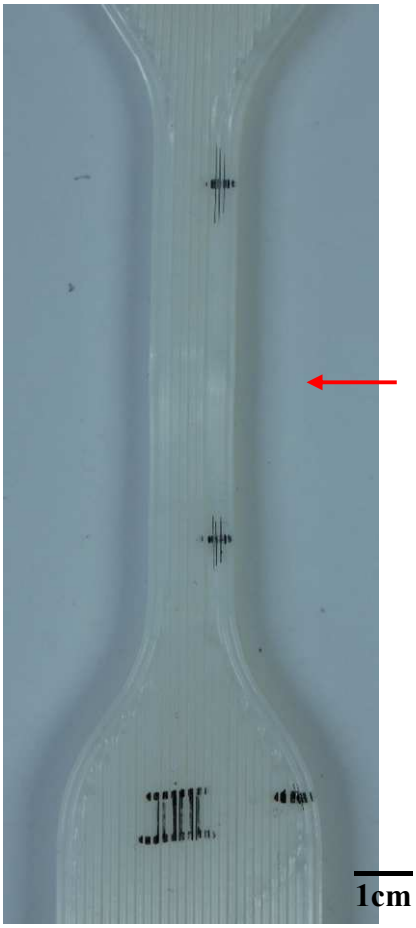

Figure 3.6.9 High mag. image of 5% TPU 90° deformation after recovery.

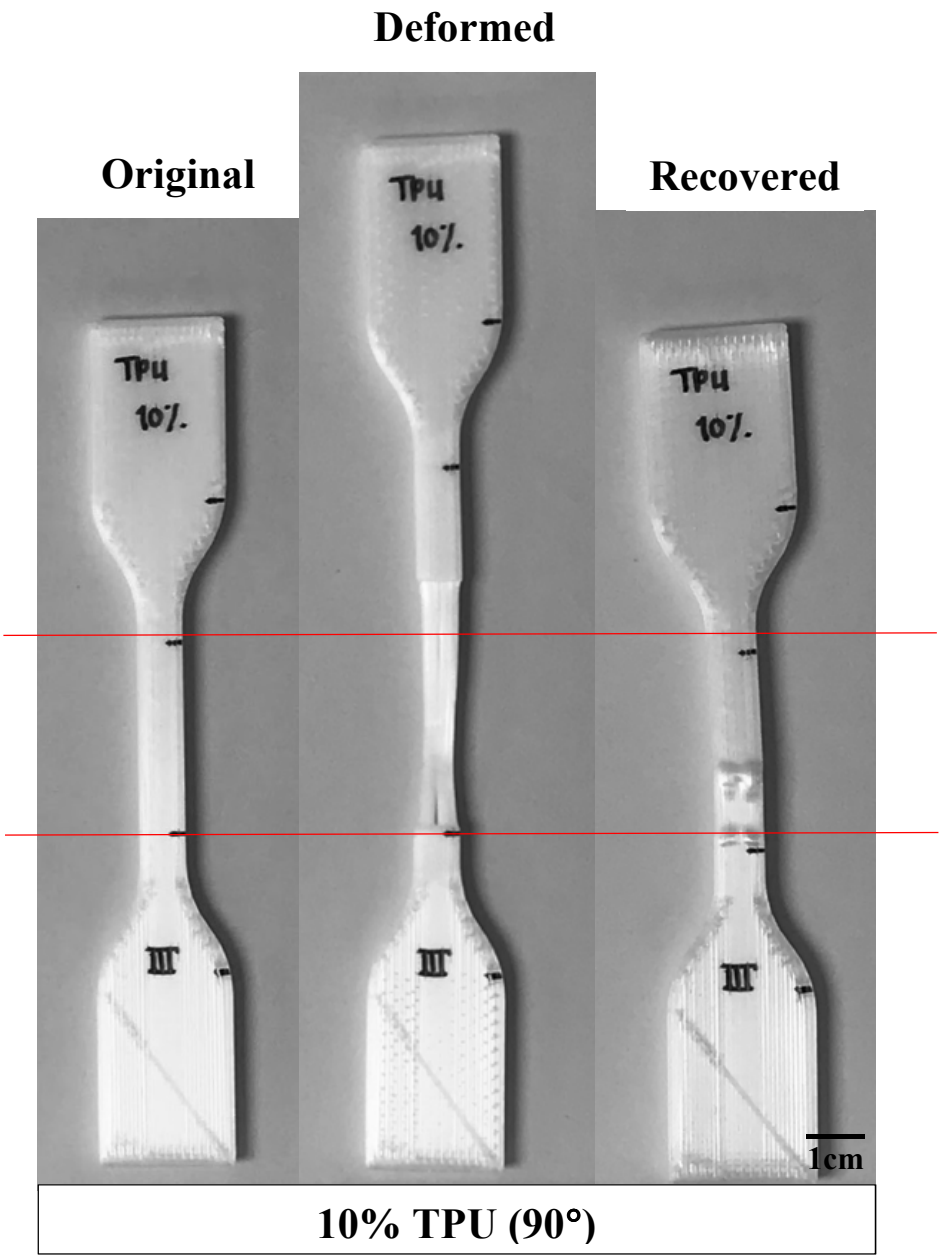

Figure 3.6.10 Photograph of 10% TPU at 90° raster pattern where the specimen was stretched to 100% elongation and partly recovered at 80°C.

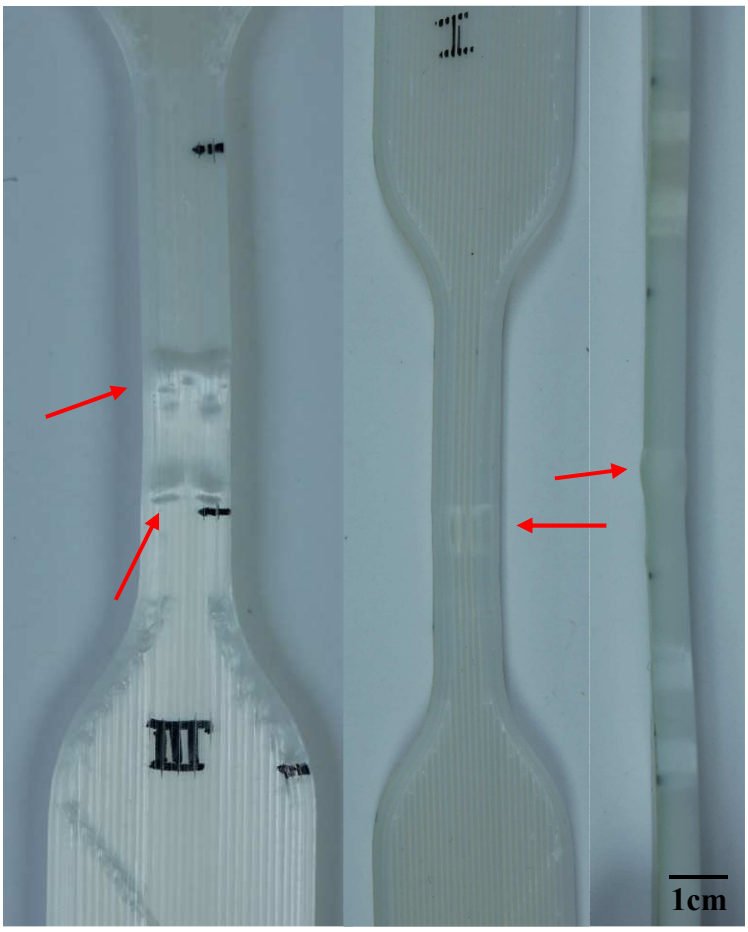

Figure 3.6.11 High mag. image of 10% TPU 90° deformation after recovery.

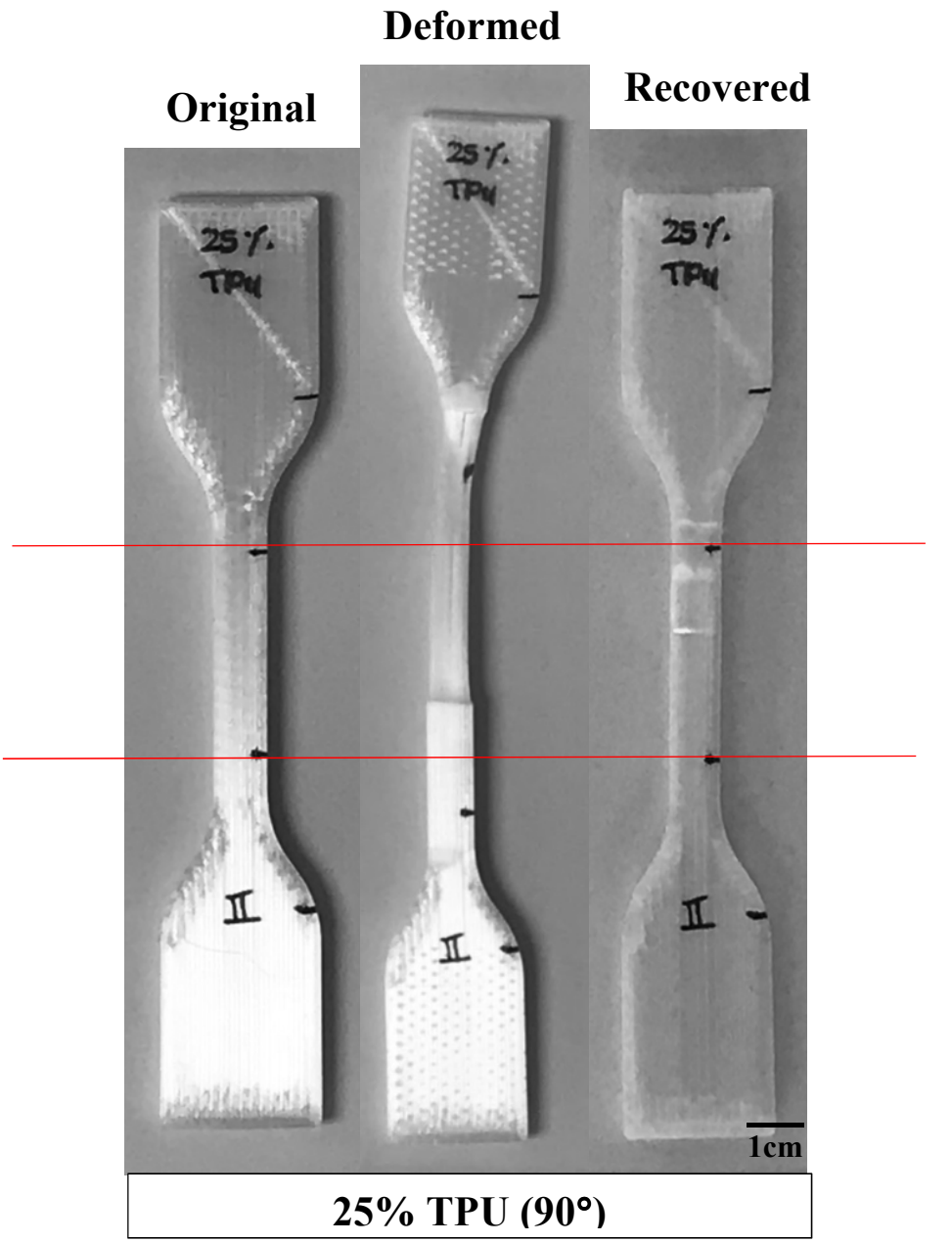

Figure 3.6.12 Photograph of 25% TPU at 90° raster pattern where the specimen was stretched to 100% elongation and partly recovered at 80°C.

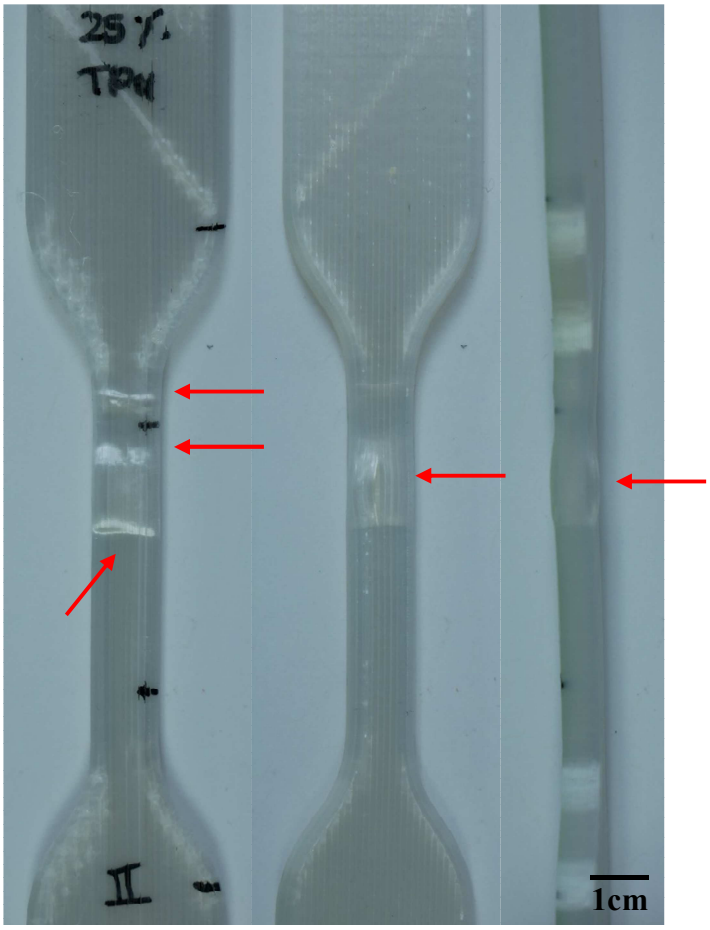

Figure 3.6.13 High mag. image of 25% TPU 90° deformation after recovery.

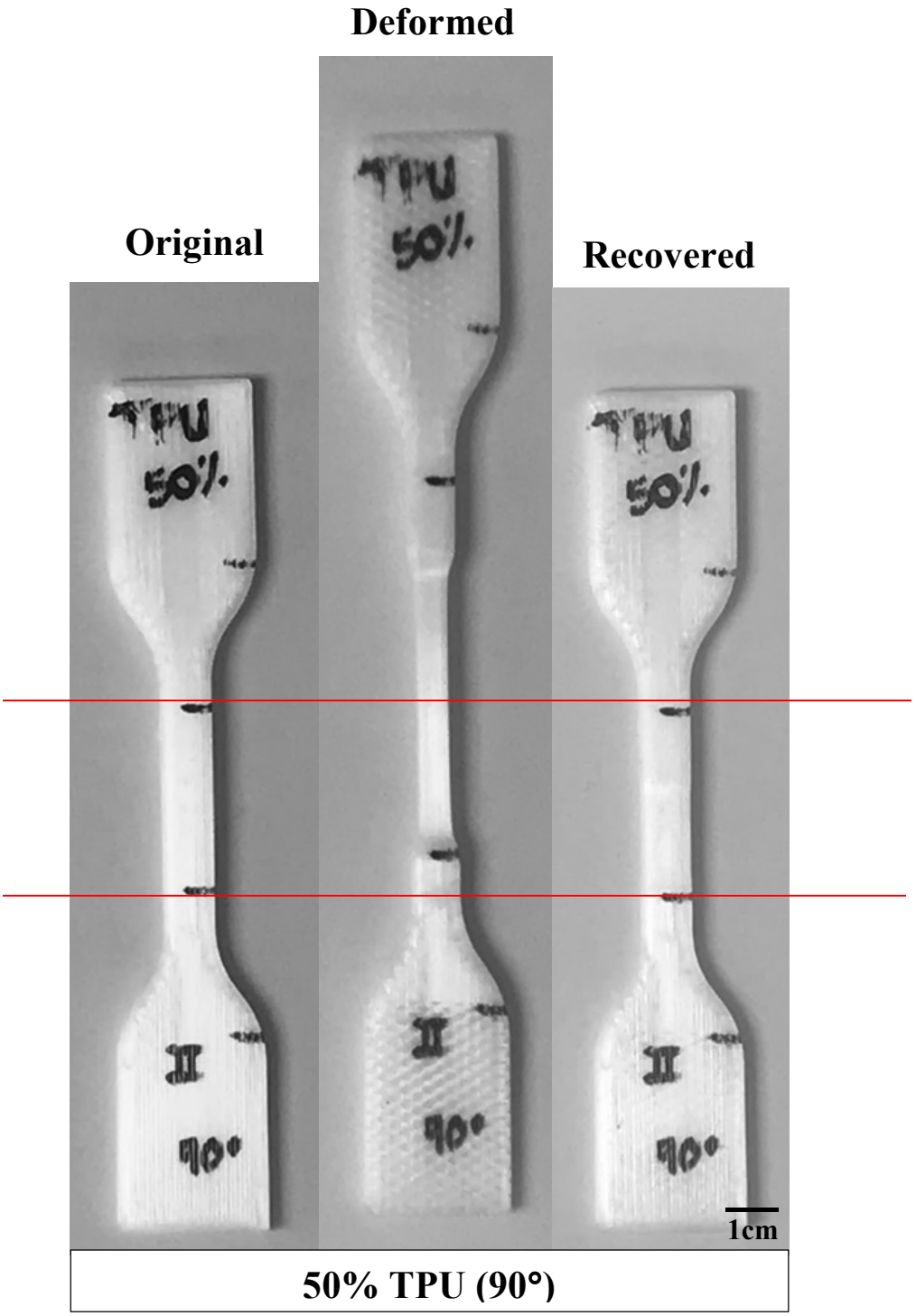

Figure 3.6.14 Photograph of 50% TPU at 90° raster pattern where the specimen was stretched to 100% elongation and partly recovered at 80°.

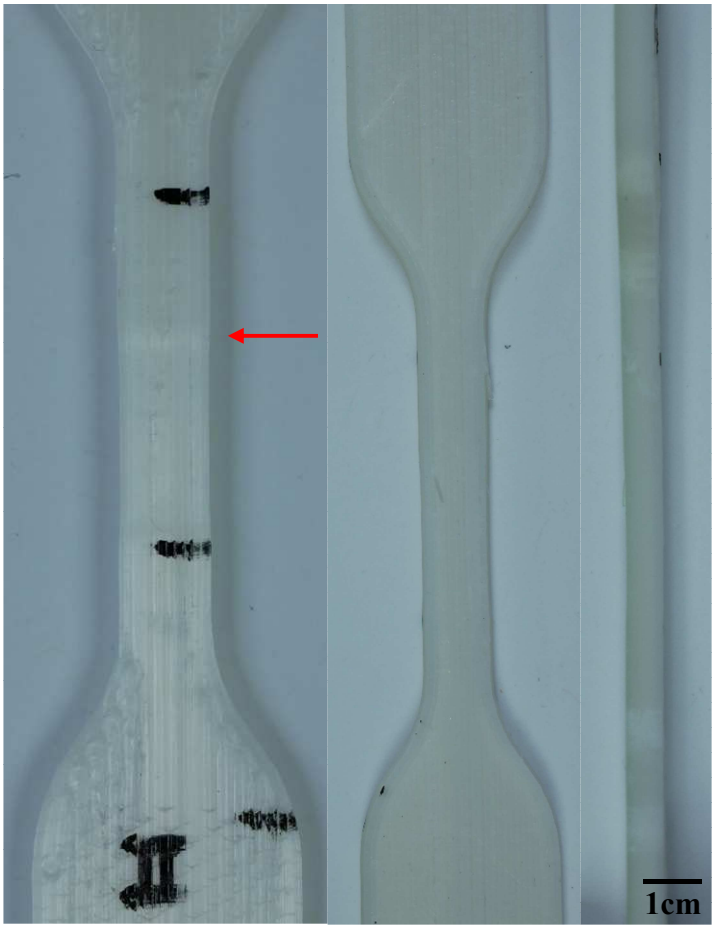

Figure 3.6.15 High mag. image of 50% TPU 90° deformation after recovery.

Chapter 4

Summary and Conclusions

4.1 DICUSSION

The results that were presented in the previous chapter indicate that shape memory recovery was successful in various blends with longitudinal and injection molding specimens. Characterization of all blends with different weight ratios help indicate the behavior of the percentages with shape memory properties. DMA illustrated that low percentage blends had a higher tan delta than the higher percentage blends for both SEBS and TPU. While TPU blends had an overall lower tan δ than SEBS blends, this is indicating of a material that is more elastic (rubbery). XRD showed that after temperature treatment the crystallinity of the material was enhance for all blends except for 10% SEBS. It is unsure why 10% SEBS did not undergo an increase in crystallinity compared to other blends. Impact testing showed that for 25% SEBS blend has the best performance in strength, resistance and break energy. While TPU 50% had the best overall performance in impact strength, resistance and break energy. It should be noted that the impact testing injection molding specimens had voids in the middle due to insufficient filling and techniques. These defects could create an issue with the actual results, the specimens were weighed to make sure that even though there were voids within some specimens the overall specimen weight was the same for all samples. The fracture surfaces of the impact specimens were analyzed by SEM. Analyzing the SEM images for 3D printed SEBS blends demonstrated an increase in plastic deformation by increasing percentage blends and 50% SEBS revealed necking. The 3D printed TPU impact specimens showed fibrils much earlier on in the material and demonstrated increasing plastic deformation with increasing weight ratio. The injection molding SEBS material

show to have an immiscible blend where you can see to phases, a brittle-ductile mode within the surface of the specimen. Figure 3.4.3 show a non-uniform surface which can be seen in 25% SEBS and even greater in 50% SEBS. TPU injection molding demonstrated similar behavior to injection molding SEBS, where we can see different fracture modes. We can see a brittle mode going to a ductile mode that shows striations in Figure 3.4.4. We also noticed fibrils in all blends. This material was quantified by using 4 different specimens of fracture surface to identify that these characteristics were shown in all surfaces of each blend.

Tensile testing for 45° raster pattern has an increase in strain percentage with increasing weight ratio percentage. Although there is a high strain, this is due to delamination and the specimens essentially fail much sooner than in noted by the graphs, which led to discarding specimen deformation for this raster pattern. Both injection molding and 90° demonstrated similar patterns in which strain percentage increased with SEBS and TPU blend percentage, respectively. A material should have strain of 50% for it to be considered for deformation. In this case only 50% SEBS, 25% TPU, 50% TPU injection molding, 50% SEBS 90° and 5%, 10%, 25% and 50% TPU 90° were the blends used for deformation at room temperature. The overall best blend after calculation was 50% TPU 90°, which would concluded that dual-component is better than dual-state for shape memory. It is intended to continue this study to determine and understand how these blends behave after several cycles of deformation and recovery. It should also be noted that 50% TPU 90° did not only demonstrate the best results overall for shape memory index, but it was also one of the only specimens that did not show any major defect in the specimen after recovery.

4.1 CONCLUSION

In conclusion, we were able to demonstrate 100% elongation and recovery in some blends at room temperature deformation with a successful outcome of regaining the materials nearly its complete original shape by heating at the tan δ temperature of 80°C. The combination of PLA with the thermoplastic rubber SEBS and TPU at different weight ratios yields a material system compatible with desktop-grade FDM™-type additive manufacturing platforms. The DMA testing process seems to induce crystallinity for some of the PLA:SEBS blends and all for the PLA:TPU blends. Tensile testing showed that not 45° rater pattern could not be deformed at room temperature without complete breakage of the specimen. While only 25% and 50% blends for SEBS injection molding and longitudinal showed signed of elongation at room temperature, as well as PLA:TPU injection molding 25% and 50% demonstrated capabilities. While PLA:TPU longitudinal showed that all blends were able to deform at room temperature. The overall best blend was 50% TPU 90° with the highest SMI out of all the blends. Here, we were able to determine that the dual component mechanism is the best for driving the shape memory effect. Combining the two mechanism allows for a stronger material that can deform at room temperature with higher weight percentages. We were successfully able to print specimens using these blends in a 3D printed as mentioned above and study their behavior in relations to SMP. The PLA;SEBS and PLA:TPU blends shows to have

References

Alan Schoener, C., Bell Weyand, C., Murthy, R. and Ann Grunlan, M. (2010), "Shape memory polymers with silicon -containing segments", *Journal of Materials Chemistry*, Vol. 20 No. 9, pp. 1787–1793.

Berman, B. (2012), "3-D printing: The new industrial revolution", *Business Horizons*, Vol. 55 No. 2, pp. 155–162.

Buyuksungur, S., Tanir, T.E., Buyuksungur, A., Irem Bektas, E., Kose, G.T., Yucel, D., Beyzadeoglu, T., et al. (2017), "3D printed poly(ε-caprolactone) scaffolds modified with hydroxyapatite and poly(propylene fumarate) and their effects on the healing of rabbit femur defects", *Biomaterials Science*, Vol. 5 No. 10, pp. 2144–2158.

Chávez, F.A., Siqueiros, J.G., Carrete, I.A., Delgado, I.L., Ritter, G.W. and Roberson, D.A. (2018), "Characterisation of phases and deformation temperature for additively manufactured shape memory polymer components fabricated from rubberised acrylonitrile butadiene styrene", *Virtual and Physical Prototyping*, Vol. 0 No. 0, pp. 1–15.

Chulilla Cano, J.L. (2011), "The Cambrian Explosion of Popular 3D Printing", *International Journal of Interactive Multimedia and Artificial Intelligence*, IMAI Software - International Journal of Interactive Multimedia and Artificial Intelligence, Vol. 1 No. 4, p. 30.

Es-Said, O.S., Foyos, J., Noorani, R., Mendelson, M., Marloth, R. and Pregger, B.A. (2000), "Effect of Layer Orientation on Mechanical Properties of Rapid Prototyped Samples", *Materials and Manufacturing Processes*, Vol. 15 No. 1, pp. 107–122.

Esposito Corcione, C., Gervaso, F., Scalera, F., Montagna, F., Sannino, A. and Maffezzoli, A.

(2017), “The feasibility of printing polylactic acid–nanohydroxyapatite composites using a low-cost fused deposition modeling 3D printer”, *J. Appl. Polym. Sci.*, Vol. 134 No. 13, p. n/a–n/a.

Hashima, K., Nishitsuji, S. and Inoue, T. (2010), “Structure-properties of super-tough PLA alloy with excellent heat resistance”, *Polymer*, Elsevier Ltd, Vol. 51 No. 17, pp. 3934–3939.

Jiang, J., Su, L., Zhang, K. and Wu, G. (2013), “Rubber-toughened PLA blends with low thermal expansion”, *Journal of Applied Polymer Science*, Vol. 128 No. 6, pp. 3993–4000.

Lai, S.-M. and Lan, Y.-C. (2013a), “Shape memory properties of melt-blended polylactic acid (PLA)/thermoplastic polyurethane (TPU) bio-based blends”, *J Polym Res*, Vol. 20 No. 5, p. 140.

Lai, S.-M. and Lan, Y.-C. (2013b), “Shape memory properties of melt-blended polylactic acid (PLA)/thermoplastic polyurethane (TPU) bio-based blends”, *J Polym Res*, Vol. 20 No. 5, p. 140.

Lendlein, A., Jiang, H., Jünger, O. and Langer, R. (2005), “Light-induced shape-memory polymers”, *Nature*, Vol. 434 No. 7035, pp. 879–882.

Luo, X. and Mather, P.T. (2013), “Design strategies for shape memory polymers”, *Current Opinion in Chemical Engineering*, Elsevier Ltd.

Memarian, F., Fereidoon, A. and Ghorbanzadeh Ahangari, M. (2018), “Effect of acrylonitrile butadiene styrene on the shape memory, mechanical, and thermal properties of thermoplastic polyurethane”, *Journal of Vinyl and Additive Technology*, Vol. 24, pp. E96–E104.

Pantoja, M., Jian, P.-Z., Cakmak, M. and Cavicchi, K.A. (2019), "Shape Memory Properties of Polystyrene- *block* -poly(ethylene- *co* -butylene)- *block* -polystyrene (SEBS) ABA Triblock Copolymer Thermoplastic Elastomers", *ACS Applied Polymer Materials*, Vol. 1 No. 3, pp. 414–424.

Peng, P., Shi, B., Jia, L. and Li, B. (2010), "Relationship between Hansen Solubility Parameters of ABS and its Homopolymer Components of PAN, PB, and PS", *Journal of Macromolecular Science, Part B*, Vol. 49 No. 5, pp. 864–869.

Peng Wu, P., Shuhua Qi, S., Nailiang Liu, N., Kangqing Deng, K. and Haiying Nie, H. (2011), "Investigation of Thermodynamic Properties of SIS, SEBS, and Naphthenic Oil by Inverse Gas Chromatography", *Journal of Elastomers & Plastics*, SAGE PublicationsSage UK: London, England, Vol. 43 No. 4, pp. 369–386.

Perez, A.R.T., Roberson, D.A. and Wicker, R.B. (2014), "Fracture Surface Analysis of 3D-Printed Tensile Specimens of Novel ABS-Based Materials", *J Fail. Anal. and Preven.*, Vol. 14 No. 3, pp. 343–353.

Roberson, D., Shemelya, C.M., MacDonald, E. and Wicker, R. (2015), "Expanding the applicability of FDM-type technologies through materials development", *Rapid Prototyping Journal*, Vol. 21 No. 2, pp. 137–143.

Roberson, D.A., Torrado Perez, A.R., Shemelya, C.M., Rivera, A., MacDonald, E. and Wicker, R.B. (2015), "Comparison of stress concentrator fabrication for 3D printed polymeric izod impact test specimens", *Additive Manufacturing*, Vol. 7, pp. 1–11.

Rocha, C.R., Perez, A.R.T., Roberson, D.A., Shemelya, C.M., MacDonald, E. and Wicker, R.B. (2014), "Novel ABS-based binary and ternary polymer blends for material extrusion 3D

printing", *Journal of Materials Research*, Vol. 29 No. 17, pp. 1859–1866.

Rocha Gutierrez, C.R. (2016), *Improving the Engineering Properties of PLA for 3D Printing and Beyond*, The University of Texas at El Paso, United States – Texas, available at: https://search.proquest.com/docview/1803936514/abstract/593F598998924A60PQ/1.

Shemelya, C., De La Rosa, A., Torrado, A.R., Yu, K., Domanowski, J., Bonacuse, P.J., Martin, R.E., et al. (2017), "Anisotropy of thermal conductivity in 3D printed polymer matrix composites for space based cube satellites", *Additive Manufacturing*, Vol. 16, pp. 186–196.

Shemelya, C.M., Rivera, A., Perez, A.T., Rocha, C., Liang, M., Yu, X., Kief, C., et al. (2015), "Mechanical, Electromagnetic, and X-ray Shielding Characterization of a 3D Printable Tungsten–Polycarbonate Polymer Matrix Composite for Space-Based Applications", *Journal of Elec Materi*, Vol. 44 No. 8, pp. 2598–2607.

Siemann, U. (1992), "The solubility parameter of poly(dl-lactic acid)", *European Polymer Journal*, Vol. 28 No. 3, pp. 293–297.

Siqueiros, J.G., Schnittker, K. and Roberson, D.A. (2016), "ABS-maleated SEBS blend as a 3D printable material", *Virtual and Physical Prototyping*, Vol. 11 No. 2, pp. 123–131.

Torrado, A.R. and Roberson, D.A. (2016), "Failure Analysis and Anisotropy Evaluation of 3D-Printed Tensile Test Specimens of Different Geometries and Print Raster Patterns", *J Fail. Anal. and Preven.*, Vol. 16 No. 1, pp. 154–164.

Torrado, A.R., Shemelya, C.M., English, J.D., Lin, Y., Wicker, R.B. and Roberson, D.A. (2015), "Characterizing the effect of additives to ABS on the mechanical property anisotropy of specimens fabricated by material extrusion 3D printing", *Additive Manufacturing*, Vol. 6,

pp. 16–29.

Vega, V., Clements, J., Lam, T., Abad, A., Fritz, B., Ula, N. and Es-Said, O.S. (2011), "The Effect of Layer Orientation on the Mechanical Properties and Microstructure of a Polymer", *J. of Materi Eng and Perform*, Vol. 20 No. 6, pp. 978–988.

Wang, C., Kou, B., Hang, Z., Zhao, X., Lu, T., Wu, Z. and Zhang, J.-P. (2018), "Pigment & Resin Technology Tunable shape recovery progress of thermoplastic polyurethane by solvents Article information:"Recent development in electrospun polymer fiber and their composites with shape memory property: a review" For Authors Tunable shape recovery progress of thermoplastic polyurethane by solvents", *Pigment & Resin Technology*, Vol. 47 No. 1, pp. 47–54.

Yang, W.G., Lu, H., Huang, W.M., Qi, H.J., Wu, X.L. and Sun, K.Y. (2014), "Advanced Shape Memory Technology to Reshape Product Design, Manufacturing and Recycling", *Polymers*, Vol. 6 No. 8, pp. 2287–2308.

Yang, Y., Chen, Y., Wei, Y. and Li, Y. (2016), "3D printing of shape memory polymer for functional part fabrication", *Int J Adv Manuf Technol*, Vol. 84 No. 9–12, pp. 2079–2095.

Zhang, W., Chen, L. and Zhang, Y. (2009), "Surprising shape-memory effect of polylactide resulted from toughening by polyamide elastomer", *Polymer*, Vol. 50 No. 5, pp. 1311–1315.

Vita

Paulina Aileen Quinonez was born on October 20, 1993 in El Paso, TX. She is the middle child and only girl to Luis F. and Lilia Quinonez. She attended Father Yermo High School for here elementary and high school in El Paso. Upon entering The University of Texas at El Paso in fall 2011, Paulina decided to get a Bachelor's of Science degree in Chemistry. She graduated in fall 2015 and worked at a supplemental instructor in El Paso Community College. Paulina has had two internships, one in Lawrence Livermore National Laboratory and the second with Lockheed Martin Space.

Chavez, F. A., Quinonez, P.A., & Roberson, D. A. (2019). Hybrid metal/thermoplastic composites for FDM-type additive manufacturing. *Journal of Thermoplastic Composite Materials*. https://doi.org/10.1177/0892705719864150

Pau.aylin@hotmail.com

This thesis/dissertation was typed by Paulina A. Quinonez.